NUREG/CR--3077

DE83 900723

NUREG/CR-3077
BMI-2030
R7

HAARM-3 Code Verification Procedure

Topical Report

Manuscript Completed: October 1981
Date Published: November 1982

Prepared by
J. A. Gieseke, K. W. Lee, H. Jordon,
H. A. Arbib

Battelle Columbus Laboratories
505 King Avenue
Columbus, OH 43201

Prepared for
Division of Accident Evaluation
Office of Nuclear Regulatory Research
U.S. Nuclear Regulatory Commission
Washington, D.C. 20555
NRC FIN A4063

TABLE OF CONTENTS

TABLE OF CONTENTS
(continued)

List of Tables

List of Figures

List of Figures
(continued)

Page

HAARM-3 CODE VERIFICATION PROCEDURE

J. A. Gieseke, K. W. Lee, H. Jordan,
and H. A. Arbib

INTRODUCTION

The purpose of this document is to recommend a procedure for experimental verification of the HAARM-3 computer code[1]. The HAARM-3 code predicts aerosol behavior within a containment vessel under assumed accident conditions for an LMFBR. Calculations are made of aerosol agglomeration (Brownian, gravitational and turbulent), deposition on walls (Brownian diffusion, thermophoresis), sedimentation onto the floor, leakage, and aerosol input from a source. Verification of the code is expected to be derived from comparisons with experimental results already available and with additional experiments to be conducted. The specific purpose of this plan is then to identify procedures, set limits for agreement, and identify experiments and measurements needed to assess the adequacy of the HAARM-3 code in predicting aerosol behavior.

The HAARM-3 code is basically a mechanistic model. It should be noted that mechanistic models have some advantages over other models such as strictly empirical models (e.g., a response expressed as an arbitrary function, such as a series, of the variables expected to predominate). Some advantages of mechanistic models are that they contribute to an understanding of the phenomena under study, provide a better basis for extrapolation of scaling, and usually require few fitting parameters.

The basis for the verification procedures developed in this document assumes that with proper choices of dimensionless groups which represent controlling mechanisms for aerosol behavior, the agreement between code prediction and experimental results provides a direct measure of the confidence one can have in code predictions for assumed accidents. The strength of this assumption is of course mitigated by uncertainties in experimental data. The procedure then provides a method for verifying the HAARM-3 code in terms of the confidence one can have in predictions for accident conditions and based on comparisons of the code with experimental data.

HAARM-3 CODE DESCRIPTION

As a necessary prerequisite for describing verification needs, the nature of the HAARM-3 code must be understood. The details of the calculational procedures and the various physical processes have been published previously[1]. Information on assumptions and mechanisms needed in formulating a verification procedure will be provided here.

General Features and Assumptions

The HAARM-3 computer code calculates the rate of collisions among airborne particles having a heterogeneous size distribution, the rate of particle deposition on the floor of an enclosed vessel, the rate of deposition of particles on the walls, the leakage of airborne particles, and the injection of particles from a source. The agglomeration growth of particles resulting from particle-particle collisions is considered to be the result of Brownian motion, differential settling velocities, and gas turbulence effects. One of the assumptions employed in the model is that the aerosol size distributions remain lognormal throughout time. However, the three size distribution parameters of the mean aerosol size, the geometric standard deviation, and the total concentration are allowed to change. In addition, the aerosol particles are assumed to be uniformly distributed within the containment.

In calculating the aerosol agglomeration and deposition rates which are dependent on the morphological properties of agglomerates, the results of a recent experimental study[2] have been utilized. The effects of nonspherical shape of the agglomerates on settling velocity and collision rate is also accounted for in the code.

The assumptions, both explicit and implicit, in the HAARM-3 code can be identified more specifically to include the following:

(1) The aerosol in an enclosure (containment vessel) is well-mixed and there are no spatial inhomogeneities for the aerosol

(2) The size distribution for the aerosol is always lognormal, although the distribution parameters may vary.

(3) Wall deposition occurs by diffusion or thermophoresis across "boundary layers" in the gas at the surfaces. These "boundary layers" are describable in terms of an average value for all deposition surfaces.

(4) Temperature gradients causing thermophoresis are uniform or describable as an average value for all surfaces.

(5) Agglomerates of sodium oxides are nearly spherical and by assuming a spherical shape, the size of the agglomerates can be corrected by using a single factor, α, that accounts for the reduced density of the porous structure. This correction factor is size dependent.

(6) Agglomerates of UO_2 particles are "chain-like". Such chain-like agglomerates fall at a rate corrected by a size independent parameter, χ, and have a projected or collision area for agglomeration corrected by a second size independent parameter, γ.

(7) Aerosol particles calculated to deposit on wall or floor surfaces remain deposited and are not resuspended.

(8) There is no attenuation of aerosol concentration during leakage from the enclosed volume.

(9) There are so few particles of large sizes that inertial effects in the gravitational agglomeration process can be neglected for the entire aerosol size distribution.

(10) Agglomeration and deposition rates are describable in terms of linear sums of the individual rate constants or deposition velocities, respectively.

Governing Equation

The governing integro-differential equation describing the rate of change of particle concentration due to various agglomeration and removal mechanisms may be written in the following form

$$\frac{\partial}{\partial t} n(x,t) = [1/2 \int_0^x \phi(\xi, x-\xi)\, n(\xi, t)\, n(x-\xi,t)\, d\xi$$

$$-n(x,t) \int_0^\infty \phi(x, \xi)\, n(\xi,t)\, d\xi \;] \qquad (1)$$

$$-n(x,t)\, R(x) + S(x,t),$$

where

$\phi(x,\xi)$ = the normalized collision kernel predicting the probability of collision between two particles of volume x and ξ due to Brownian motion, gravitational settling, and turbulent gas motion

$x = \frac{4}{3} \pi r_1^3$ = volume of particle with radius r_1

$\xi = \frac{4}{3} \pi r_2^3$ = volume of particle with radius r_2

t = time

$n(x,t)$ = the number density distribution

$R(x)$ = the removal rate of particles by gravitational settling to the floor, diffusion to the walls (wall plating), and leakage

$S(x,t)$ = represents the source rate of particles input to the vessel.

The first integral in Equation (1) represents the formation rate of particles between the sizes x and x + dx as a result of collisions

between particles of volumes ξ and $x - \xi$. Similarly, the second integral represents the disappearance rate of particles in the size range between x and x + dx due to collisions with all other particles.

The functional form of the collision kernel $\phi\ (x,\xi)$ depends upon the coagulation mechanisms present in a given system. In an enclosed containment vessel, possible mechanisms causing relative motion between particles, and thus coagulation, include Brownian motion of the particles, gravitational settling, and turbulent gas motion. In most analyses where more than one of these mechanisms are present, they are assumed to be separable and additive such that

$$\phi\ (x,\xi) = K_B(x,\xi) + K_G(x,\xi) + K_T(x,\xi). \tag{2}$$

Agglomeration Terms

Brownian

Current aerosol models use the Brownian collision parameter in a form which can be written as

$$K_B(r_1,r_2) = \frac{K_o}{2}\ (r_1 + r_2)\left[\left(\frac{1}{r_1} + \frac{1}{r_2}\right) + \alpha^{1/3}\ C_m \lambda \left(\frac{1}{r_1^2} + \frac{1}{r_2^2}\right)\right]\frac{\gamma}{\chi}\ , \tag{3}$$

where $K_o = 4kT/3\eta$ = the agglomeration rate constant

k = the Boltzmann constant

T = the gas temperature

η = the gas viscosity.

Further, C_m is constant defining the Cunningham correction factor which accounts for the low Knudsen number effects present for small particles, α is the density correction factor, γ collision shape factor, χ dynamic shape factor, and λ is the gas mean free path. The nature of α is described and discussed in a previous report[3].

Gravitational

The collision parameter for gravitational agglomeration is based on consideration of the relative sedimentation rates for different sized particles and is dependent on the collection of small particles from the volume swept out by a large, rapidly settling particle. A general expression for the gravitational collision parameter will be presented and deviations from this used in the various models discussed. The gravitational agglomeration parameter is given by

$$K_G(r_1,r_2) = \varepsilon(r_1,r_2)\,\frac{2\pi g\rho}{9\eta}\left[\alpha^{-1/3}(r_1 + r_2)^3|r_1 - r_2| + C_m\lambda(r_1 + r_2)^2|r_1 - r_2|\right]\frac{\gamma^2}{\chi} \tag{4}$$

where

$\varepsilon(r_1,r_2)$ = the particle-particle collision efficiency
ρ = the particle density
g = gravitational constant.

Turbulent

Particles can also be caused to collide in a turbulent gas by being suspended in a shear flow and by inertial effects causing relative motion between particles. These agglomeration rates have been previously[1] shown to be

$$\begin{aligned} K_T(r_1,r_2) = {} & \varepsilon(r_1,r_2)\left(\frac{8\pi\varepsilon_T\rho_g}{15\eta}\right)^{1/2}\gamma^3\,\alpha^{-1}(r_1+r_2)^3 \\ & + \varepsilon(r_1,r_2)\left(\frac{4\rho\sqrt{2\pi}}{9\eta}\right)\left(\frac{1.69\varepsilon_T{}^3\rho_g}{\eta}\right)^{1/4} \\ & \cdot\left|(\alpha^{-1/3}\,r_1^2 + C_m\lambda r_1) - (\alpha^{-1/3}\,r_2^2 + C_m\lambda r_2)\right| \\ & \cdot (r_1+r_2)^2\left(\frac{\gamma^2}{\chi}\right) \end{aligned} \tag{5}$$

where

ε_T = turbulent energy dissipation rate

C_m = the constant defining the slip correction factor when the factor is approximated with two terms

ρ_g = the gas density.

Removal Terms

In Equation (1), R(x) represents the removal terms. The HAARM-3 code accounts for the four possible mechanisms: (1) removal at the vessel floor due to gravitational settling, (2) diffusion to the walls, (3) thermophoresis to the walls, and (4) leakage out of the vessel. Mathematically formulated this is

$$R(r) = G_R \left[\alpha^{1/3} r^2 + C_m\lambda\, \alpha^{2/3} r\right] \frac{1}{\chi} + P_R \left[\frac{\alpha}{r}^{1/3} + C_m\lambda\alpha^{2/3} \left(\frac{1}{r^2}\right)\right] \frac{1}{\chi} + T_R \left[\frac{1}{1 + 2C_m\lambda/(fr)}\right]\left[\frac{C_t\lambda/(fr) + k_f/k_s}{1 + 2C_t\lambda/(fr) + 2k_f/k_s}\right] \frac{1}{\chi} + R_L \tag{6}$$

where

$$G_R = \frac{2g\rho A_f}{9\ \eta V}\ , \text{ the gravitational settling constant} \tag{7}$$

$$P_R = \frac{kTA_w}{6\pi\eta V\Delta}\ , \text{ the wall plating diffusional constant} \tag{8}$$

$$T_R = \frac{3\eta A_w \nabla T}{2\rho_g \overline{VT}}, \text{ the wall plating thermophoresis constant} \tag{9}$$

R_L = leak rate from the vessel

Δ = diffusion boundary layer thickness

V = the vessel volume

C_t = coefficient for thermal accommodation at the particle surface

k_f/k_s = ratio of gas to particle thermal conductivity

λ = mean free path of gas molecules

∇T = the temperature gradient at the wall

A_f = area of the vessel floor
A_w = area of the vessel wall
$f = \alpha^{-1/3}$.

Solution Technique

In order to solve Equation (1), the technique called "method of moments" is utilized in the HAARM-3 code. By assuming that the aerosol size distribution remains lognormal, it is possible to convert the integro differential equation into a set of simple first order differential equations. The details of the solution technique can be referred to previous reports[1,4-6] and will not be described here.

GENERAL APPROACH TO VERIFICATION

It is important to recognize that verification of the HAARM-3 code means that the suitability of the code for predicting aerosol behavior under conditions assumed or believed to be existing during an accident is established through experimental means. Because the HAARM-3 code is mechanistic in nature, it must be demonstrated that the code adequately describes the physical processes or mechanisms which occur and that the code is applicable to the expected or assumed accident situations. In other words, it is not sufficient to only verify the adequacy of the model describing an individual mechanism or process under arbitrary conditions, but it must be shown that the code in fact predicts aerosol behavior under expected realistic conditions in which processes interact or compete and in which mechanisms possibly not included in the overall model might have an influence.

The above considerations suggest that an important step in code verification is to assess the possible boundaries or ranges for variables and conditions. In addition, the requirements for verification become more explicit. Experimental verification should demonstrate that:

(1) The individual mechanisms or processes affecting aerosol behavior are adequately described analytically

(2) All significant mechanisms are included

(3) Interactions among individual mechanisms or processes are properly described.

Of course, the above three points must be demonstrated over the range of expected accident conditions.

In a general sense any mechanistic model is the result of a cycle or cycles in which the elements are formation of a hypothesis, design of verification tests, experimental measurements, and analysis. This cycle can also be termed developmental verification where the results of experiments can be used to improve the model as well as to verify its adequacy. Presumably, much of the developmental activities for the HAARM-3 code are completed through prior comparisons with experimental results. (For example, the incorporation of gravitational agglomeration as a particle growth mechanism was based on the observed inability of codes to predict aerosol behavior when this mechanism was excluded.) The major task at this time is more strictly verification rather than development. Figure 1 represents the logic sequence to be used in the verification process. A "recycle" arrow connecting experimental results to code modification represents a developmental activity that may or may not be required depending on the ability of the HAARM-3 code to predict experimental results.

The features of the verification process as shown in Figure 1 are then to establish by sensitivity analyses the most important variables affecting code output, to specify experiments which will investigate the ability of the code to predict the effects of changes in these variables, and to analyze the results to determine if the code predictions are suitably in agreement with the experimental results.

A critical feature of the code verification process is the establishing of criteria by which to assess whether the code predictions are adequately accurate. These criteria relate to both the need for accuracy in the code prediction and the accuracy of the experimental data. The

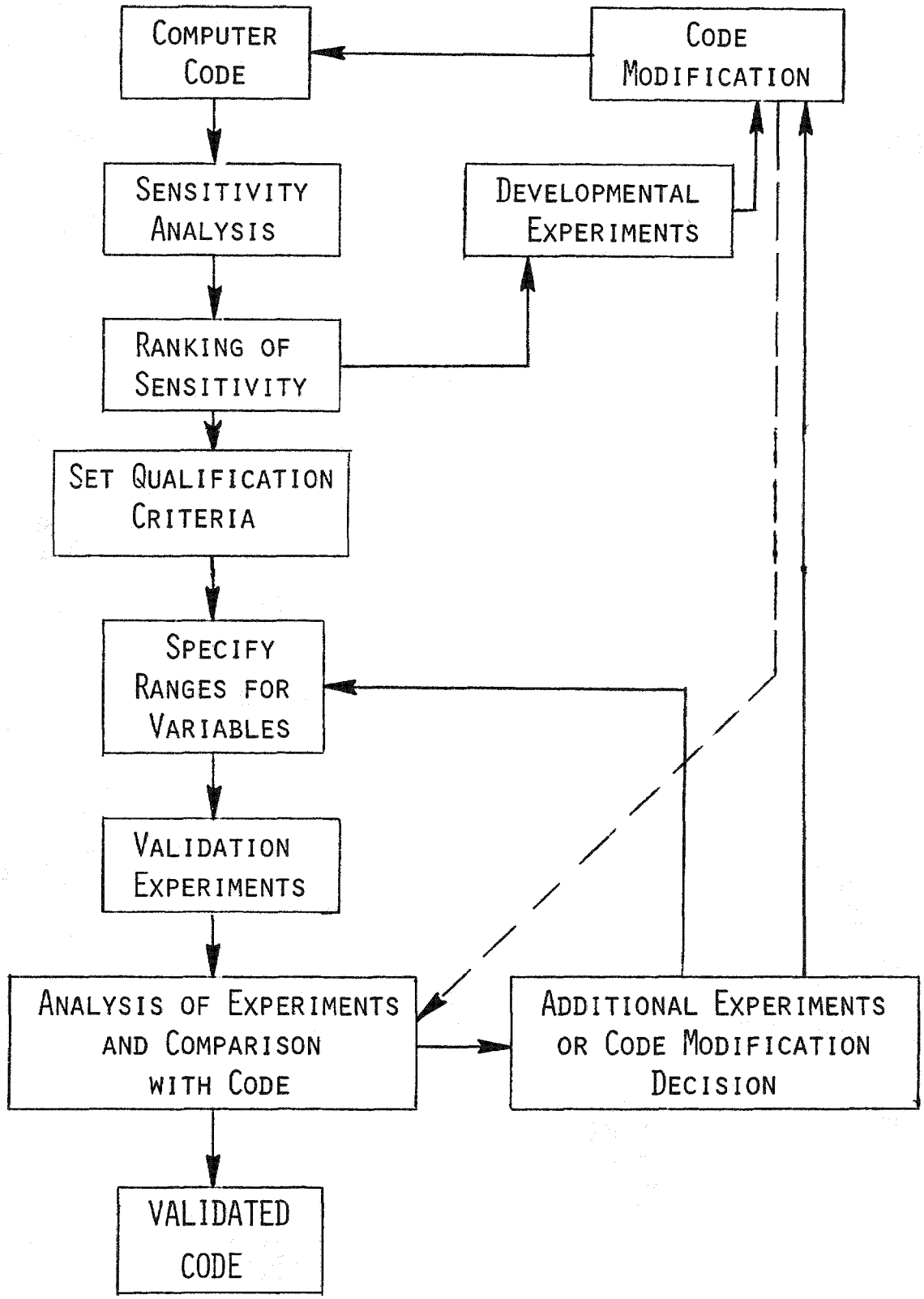

FIGURE 1. CODE VERIFICATION PROCESS

use of the HAARM-3 code in licensing procedures or risk assessments suggests that the code will be adequate if it can predict within a factor of two or three the actual mass leakage from a containment vessel assuming no attenuation in the leak path. Since the leakage rate and time may be arbitrary, this means that airborne concentration predictions within a factor of about two are adequate.

Such a comparison, of course, is complicated by the fact that there may exist certain experimental errors combined with inherent data spreads among measurements. The computer code is deterministic but there are uncertainties associated with the values for the inputs and model parameters, as illustrated in Figure 2, therefore, there exist two separate distributions; one for experimental data and the other one for computer runs. It is therefore decided that certain statistical means be employed for validating the HAARM-3 computer code. For the statistical analysis, the airborne particle concentration will be used as a reference since the leakage rate that is expected in a hypothetical accident can directly be related to the airborne concentration. The basic question of whether the values predicted by the theoretical model are consistent with the experimentally measured values will be resolved by employing a test method based on statistics. Thus, the testing method will give the level of significance with which the theoretical model can predict the experimental data. A statistical analysis such as the student t-test, the Wilcoxon rank sum statistics combined with the union-intersection principle or the two-way analysis of variance method will be considered for such a testing method. The statistical analysis will be made for the regime between the time at which the mass concentration is maximal and the time at which the concentration is approximately three orders of magnitude below the maximum. This time regime is selected due to uncertainty in the source term at times preceding the point where mass airborne concentration is maximum; and from the consideration that beyond the point in time where the concentration is below 1/1000 of the maximum, the mass airborne concentration is negligible in terms of its total contribution to actual mass leakage from the containment vessel.

In a similar fashion it is desirable to compare code predicted particle sizes with experimental measurements. Particle sizes are important because aerosol behavior mechanisms are size dependent. Comparisons will be

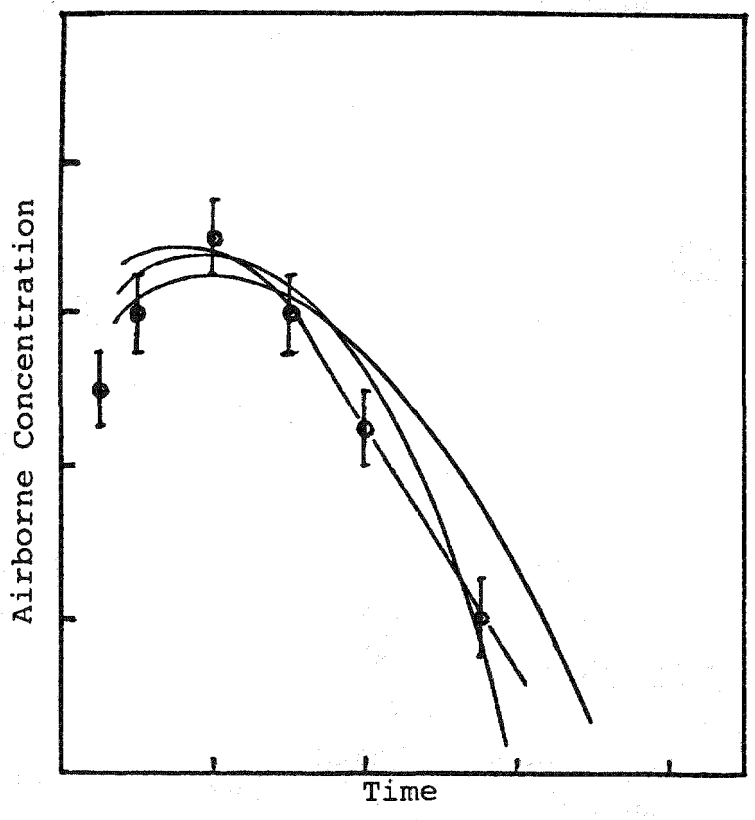

FIGURE 2. SCHEMATIC DIAGRAM SHOWING THE SPREADS OF BOTH EXPERIMENTAL DATA AND COMPUTER CALCULATIONS

based on mean aerodynamic particle size since this size is the one most often measured experimentally (by cascade impactors or spiral centrifuges) and the HAARM-3 code provides output directly as aerodynamic size. An assessment will be made regarding the extent to which calculations will predict the experimental data.

SPECIFICATION OF VARIABLE RANGES FOR ASSUMED ACCIDENT CONDITIONS

The experimental conditions chosen for use in the code validation process should reflect the ranges expected for variables under assumed accident conditions. This is important first, because the code should be verified for conditions that it is expected to represent, and second, the restriction or emphasis of selected conditions will avoid costly experiments performed under conditions of lesser pertinence. It is of benefit, then, to estimate the conditions predicted for various assumed accidents in large scale reactors. The FFTF, CRBR, Super Phenix and AI 1000 MWe designs and postulated accidents have been considered.

The reactor containment geometries and maximum potential mass concentrations are shown in Table 1. The geometries were estimated from various published figures and approximate drawings. The mass release rates were estimated to be maximum values. The release of fuel material, estimated to be between 1 and 10 percent of the fuel was taken arbitrarily as 4 percent. The continuing aerosol sources assumed that sodium would burn at the indicated rates over the indicated time periods. However, it is expected that because of aerosol deposition by the various mechanisms, maximum concentrations would not exceed about 150 to 200 g/m^3 for extended-time sources. Nevertheless, the maximum potential concentrations are noted in the table and as will be seen, somewhat lower but still quite high maximums have been assumed and a range from this maximum concentration downward has been used in evaluating expected ranges of conditions.

TABLE 1. ESTIMATED CONDITIONS FOR ASSUMED ACCIDENTS IN SELECTED REACTOR VOLUMES

Vessel/Reactor	Ident. No.	Volume, m^3	A_F/V, m^{-1}	A_W/V, m^{-1}	Mass Input Rate[a], kg/sec	Mass Input Time	Total Mass, kg	Max Potent. Mass Conc., g/m^3
CRBR:								
Head Cavity	1	7.1×10^2	2.5×10^{-1}	8.7×10^{-1}	Initial: 200 kg fuel 4000 kg Na_2O_x Continuing Na_2O_x: 1 kg/sec	Initial: Instantaneous Continuing: 50 hrs	1.8×10^5 (assumes all Na burns)	2.5×10^5 (282 fuel)
Containment	2	1.05×10^5	2.6×10^{-2}	1.1×10^{-1}	Same as head cavity above	Same as above	Same as above	1.72×10^3 (~150 can be achieved at steady state) (1.9 fuel)
Confinement (Annulus)	3	1.8×10^4	1.52×10^{-1}	1.09	1.8×10^{-4} (est'd by 0.1%/day flow of 150 g/m^3)	~75 hrs	49	2.7
FFTF: Containment	4	4.2×10^4	3.57×10^{-2}	1.21×10^{-1}	Initial: 120 kg fuel 400 kg Na_2O_x Continuing Na_2O_x: 0.15-1.3 kg/sec	20 hrs	9.4×10^4 (assumes all Na burns)	2.24×10^3 (2.86 fuel)
Super Phenix:								
Inner Containment	5	~1.8×10^4	3.6×10^{-2}	2.0×10^{-1}	Initial: 880 kg fuel Na Fire: 0.7 kg/sec	2 hrs	5.9×10^3 (based on O_2 available, 7.4% of spilled Na assumed to burn; 7.9×10^4 if all Na burns)	330 (4500 if all Na burns) (49 fuel)
Confinement Bldg.	6	2.6×10^5	1.45×10^{-2}	8.67×10^{-2}	Same as inner containment	Same as inner containment	7.9×10^4 (assumes all Na burns)	304 (3.4 fuel)
AI Design, 1000 MWe:								
Head Cavity (Open)	7	6.3×10^3	1.3×10^{-1}	1.83×10^{-1}	Variable source rate	~30 hrs	3.7×10^5	6×10^4 (~6×10^3 fuel)
Containment	8	8.5×10^4	3.125×10^{-2}	1.02×10^{-1}	Leak from head cavity	~30 hrs	3.7×10^5	4000
Confinement	9	3.0×10^4	8.32×10^{-3}	1.16	Leak from containment	~30 hrs	3.7×10^5	1.2×10^4

(a) Four percent of fuel assumed as initial source.

RESULTS OF SENSITIVITY ANALYSIS

A methodology to perform a sensitivity analysis of the HAARM-3 computer code was developed and used to study the effects on aerosol behavior of various independent variables of the code, such as initial aerosol properties and containment geometry[7]. By varying these independent variables and observing the change in results calculated with the computer code, one can analyze the sensitiveness of the aerosol behavior to various variables. Thus, the sensitivity of a computer model may be defined as a measure of change in output variables to variation in input variables. It should be noted that results from a sensitivity study of a computer model do not necessarily provide the actual sensitivity of aerosol behavior itself. Nevertheless, when the computer model is assumed sufficiently accurate, the analysis results can be useful in estimating the effects of various parameters on the actual aerosol behavior. In addition, results of such a sensitivity study will play a significant role in guiding future experimental programs intended to validate and improve the computer model and in studying optimal containment design features.

In the study, first order sensitivities of leaked mass to individual variables were calculated by running the HAARM-3 computer code based on the one-at-a-time (OAT) design. Depending on the results of this first order sensitivity calculation, higher order sensitivities of significant value were also obtained. By assuming that the range of each variable used in the analysis was established with the same confidence interval, the importance of each individual input variable and model parameter was ranked. Table 2 lists the variables or parameters considered in the analysis plus their values for the baseline case and their ranges. Table 3 shows the calculated results of the first order sensitivities of leaked aerosol mass, $\partial y/\partial x_i$ and variations in the output, Δy. The symbols used in Table 3 are as follows and the output is in μg of leaked aerosol mass:

(1) SO: source rate, no. of particles/cc-sec

(2) RSOR: mass median particle radius, μm

(3) SIGSOR: geometric standard deviation

TABLE 2. BASELINE AND THE RANGE OF VARIABLES USED IN SENSITIVITY ANALYSIS OF THE HAARM-3 CODE

	Variables/Parameters	Base Case	Range
1.	Source rate, #/cc sec	5×10^{5}	5×10^{8} - 5×10^{3}
2.	R_{50}, μm	0.5	1.0 - 0.05
3.	Geometric standard deviation, σ_g	1.5	2.5 - 1.2
4.	Source cutoff time, sec	100	1000 - 10
5.	Aerosol density, g/cm^3	2.27	10 - 1
6.	AWOV, cm^{-1}	1.1×10^{-3}	8.8×10^{-2} - 5.5×10^{-4}
7.	AFOV, cm^{-1}	2.4×10^{-4}	2.1×10^{-2} - 1.2×10^{-4}
8.	Temperature, K	320	500 - 273
9.	Diffusion boundary layer, cm	1×10^{-3}	1×10^{-2} - 5×10^{-5}
10.	Temperature gradient, K/cm	40	200 - 0
11.	Leak rate, percent/day	0.1	0.5 - 0
12.	Pressure, $dynes/cm^2$	1.012×10^{6}	2.024×10^{6} - 1.012×10^{6}
13.	Turbulent energy dissp. rate, cm^2/sec^3	0	3000 - 0
14.	Collision efficiency, ε	Variable	1 - 0.001
15.	Density correction factor, α	Variable	1 - 0.01
16.	Collision shape factor, γ	1	10 - 1
17.	Coefficient for Cunningham slip, C_m	1.37	1.8 - 1

TABLE 3. CALCULATION RESULTS OF FIRST ORDER SENSITIVITIES

Rank	Variable/ Parameter	Δy, μg	$\frac{\partial y}{\partial x_i}$
1	RVL	6.928×10^{8}	1.197×10^{16}
2	EFF	-4.988×10^{8}	-5.038×10^{8}
3	TAUIN	2.187×10^{8}	2.209×10^{5}
4	RSOR	1.771×10^{8}	1.807×10^{8}
5	SO	1.532×10^{8}	3.067×10^{1}
6	GAMMA	-1.338×10^{8}	-1.487×10^{7}
7	EPST	-1.204×10^{8}	-4.013×10^{4}
8	ALPHA	1.122×10^{8}	1.123×10^{8}
9	AFOV	-1.066×10^{8}	-5.105×10^{9}
10	RHO	9.96×10^{7}	1.107×10^{7}
11	SIGSOR	-8.232×10^{7}	-6.332×10^{7}
12	P	6.08×10^{7}	2.014×10^{1}
13	TEMP	-2.14×10^{7}	-9.427×10^{4}
14	AWOV	-1.7×10^{7}	-1.944×10^{8}
15	CM	-3.5×10^{6}	-4.375×10^{6}
16	TGRADW	-1.2×10^{6}	-6.000×10^{3}
17	DELTA	0.0	0.0

(4) TAUIN: source duration time, sec

(5) RHO: aerosol density, g/cm^3

(6) AWOV: ratio of wall area to vessel volume, cm^{-1}

(7) AFOV: ratio of floor area to vessel volume, cm^{-1}

(8) TEMP: vessel temperature, K

(9) DELTA: diffusion boundary layer, cm

(10) TGRADW: temperature gradient at wall, K/cm

(11) RVL: leakage rate, fraction of vessel volume/sec

(12) P: vessel pressure, $dyne/cm^2$

(13) EPST: turbulent energy dissipation rate, cm^2/sec^3

(14) GAMMA: collision shape factor

(15) ALPHA: density correction factor

(16) EFF: collision efficiency

(17) CM: the second coefficient in the slip correction factor.

The calculated sensitivities have been ranked and listed in decending order in Table 3. It is seen that the leakage rate, source duration time, the mean size of source aerosol, and source rate are found to increase the leaked mass most effectively. Since the leaked mass is linearly related to the leakage flow rate and suspended aerosol concentration, and since source duration time, mean size of source aerosol, and source rate are all related to a postulated accident situation, it can be said that the amount of aerosols leaked into the environment is strongly dependent upon the leak rate and the accident conditions. It is also found that increasing particle collision efficiency, collision shape factor, or turbulent energy dissipation rate are most effective in reducing the leaked mass. It is interesting to note that all these highly ranked input variables are those which control the rate of aerosol agglomeration. However, ALPHA and AFOV tend to cause the leaked mass to increase to an only moderate extent. Diffusion boundary layer thickness, wall temperature gradient, slip correction factor, and AWOV are shown to be among those which affect the aerosol behavior the least. With the exception of CM, these are the parameters which affect the various aerosol wall deposition mechanisms.

As a result of the calculated first order sensitivities and higher sensitivities of the significant values the following conclusions were drawn in the study:

(1) The results of the first order sensitivities show that (1) leak rate, (2) collision efficiency, (3) source duration time, (4) particle size, (5) source rate, (6) collision shape factor, (7) turbulent energy dissipation rate, (8) density correction factor, and (9) the area ratio of floor to wall can significantly affect the code output in that order. Considering that the calculated sensitivities of the above variables are all of the same order of magnitude, and since the sensitivities can vary somewhat depending on the choice of range for the variables, the exact order established in the given list might alter to a certain extent.

(2) Among the various input variables, leakage rate, source particle size and source rate have been found to influence most the output of HAARM-3 computer code. These input variables are directly related to accident conditions, and therefore, the importance of accident situation postulations has been shown.

(3) Among the various model parameters, those which govern the rate of aerosol agglomeration are found to be important. Particle collision efficiency, collision shape factor and turbulent energy dissipation rate have been identified to belong to this category. Further, it can be said that high values of these parameters cause the amount of leaked material to be reduced.

(4) The input variables and model parameters that are related to the aerosol deposition mechanisms do not greatly influence the amount of aerosol leaked from the containment.

(5) Calculation results of two-way interactions show that the pairs: source rate and source duration time, leak rate and source duration time, and mean particle size and source duration time, are among the most significant interactions in increasing the predicted leaked mass.

It should be noted that the above conclusions are valid only in the neighborhood of conditions represented by the baseline case values for the parameters as given previously in Table 2. Deviations from these conditions may lead to differing conclusions. However, a smaller scale sensitivity analysis performed at a new baseline mass concentration of one order of magnitude higher than the Table 2 values did not change the major conclusions. In this evaluation the effects of leak rate, collision efficiency (ϵ), turbulent energy dissipation rate (ϵ_T), collision cross-section (γ), and density correction factor (α) were nearly identical to previous values. One would expect that the importance of factors affecting wall deposition would be significantly increased if the baseline geometry were reduced to the scale of most experimental vessels and therefore the sensitivities presented here are not valid for experimental studies.

METHODOLOGY FOR SPECIFYING EXPERIMENTAL CONDITIONS FOR CODE VERIFICATION

As discussed previously, the present HAARM-3 computer code employs various aerosol behavior mechanisms involving a great number of input variables and model parameters. In addition, the code was developed based on many assumptions. A thorough and complete validation of the code for each variable and model parameter would involve numerous developmental experiments and validation experiments, and would likely require excessive costs and time. It is then obvious that a certain systematic procedure must be formulated in order to simplify the code validation plan.

The first consideration which should be taken into account in such a procedure is that all the important input variables that were found from the sensitivity analysis to significantly affect the aerosol behavior be properly varied over the range of accident conditions, and the results of such experiments and the computer calculations be compared.

The second consideration in the procedure is to provide proper accounting for the effects of scaling of various aerosol behavior mechanisms. Although the HAARM-3 computer code is to be used ultimately for predicting aerosol behavior in full scale vessels, experiments for validating the code are performed in various smaller-scaled facilities. Therefore, such experiments must be designed, performed and interpreted based on a certain strategy. Similitude between the small-scale and full-scale situations must be properly satisfied. The most convenient and simplest approach is to seek various dimensionless terms which govern aerosol behavior. Since one of the objectives of the planned code validation experiments is to verify the soundness of important aerosol mechanisms, the corresponding dimensionless terms representing these mechanisms are to be obtained. This approach is useful for evaluating the adequacy of individual and combined basic mechanisms. In addition, there are special considerations related to the assumed accident scenarios and conditions which must be taken into account. These approaches for mechanism and special considerations are to be discussed.

Procedures for Individual and Combined Basic Mechanisms

As discussed, individual aerosol behavior mechanisms employed in the HAARM-3 computer code can best be validated by developing a procedure in which the relative importance of various aerosol behavior mechanisms is comprehensively evaluated. The approach taken here is similar to that reported by Okuyama, et al[8]; however, their procedure has been expanded to consider a total of six different aerosol behavior mechanisms taken in groups of three. The first group considers the relative importance of coagulation, sedimentation and diffusion to walls. The second group concerns the three major agglomeration mechanisms and the final group concerns the relative importance of mechanisms for removing aerosols.

Okuyama, et al., originally suggested the following three dimensionless terms which control agglomeration and gravitational and diffusional deposition:

Coagulation vs. Sedimentation:
$$CG = \frac{K_o n_o C}{v_t/H} \tag{10}$$

Diffusion vs. Sedimentation
$$DG = \frac{DA_w/V\Delta}{v_t/H} \tag{11}$$

Coagulation vs. Diffusion:
$$CD = \frac{K_o n_o C}{DA_w/V\Delta} \quad ; \tag{12}$$

where

K_o = agglomeration constant
n_o = initial aerosol number concentration
C = Cunningham slip correction factor
r_{go} = initial geometric number median radius
v_t = terminal settling velocity
H = vessel height
V = vessel volume

D = diffusion coefficient

A_w = vessel wall area

Δ = wall plating parameter (diffusion layer thickness).

Figure 3 shows the various regimes where each individual mechanism is predominant. By conducting the experiments which are designed corresponding to the regimes shown in Figure 3, the important aerosol behavior mechanisms will be verified. It should be pointed out that the aerosol behavior mechanisms not included in the discussion, including thermophoresis and gravitational or turbulent agglomeration should also be validated using similar considerations. Procedures for evaluating the relative importance of the several deposition mechanisms and of the several agglomeration mechanisms are developed in the following sections.

Procedure for Evaluating Importance of Agglomeration Mechanisms

Agglomeration mechanisms and factors affecting agglomeration were found to be important from the sensitivity analysis[7], and hence, it is desirable to validate each agglomeration mechanism included in the HAARM-3 separately. Currently the HAARM-3 code contains three agglomeration mechanisms: Brownian, gravitational and turbulent agglomeration; and a procedure needed to validate these separate agglomeration mechanism is provided here.

The integro-differential equation governing the three agglomeration mechanisms can be written without the source and removal terms as

$$\frac{\partial n(x,t)}{\partial t} = \frac{1}{2} \int_0^x n(\xi,t)\, n(x-\xi,t)\, \phi(\xi,x-\xi)\, d\xi - n(x,t) \int_0^\infty n(\xi,t)\, \phi(x,\xi)\, d\xi \,. \qquad (13)$$

The three agglomeration rate kernels are assumed to be additive as given by Equation (2). The three rate kernels, K_B, K_G and K_T are defined by Equations (3) to (5), respectively.

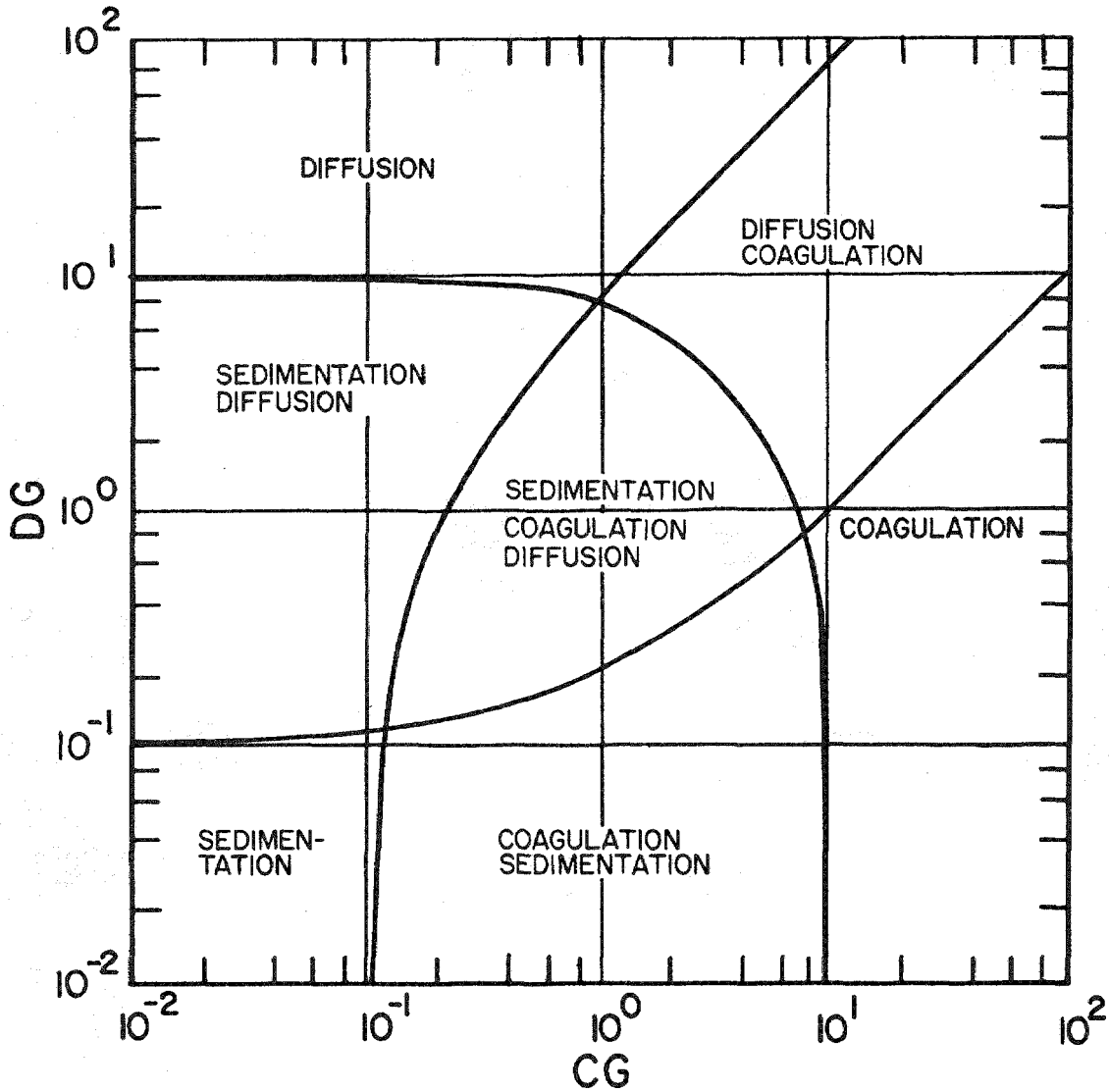

FIGURE 3. REGIMES OF PREDOMINANCE FOR VARIOUS AEROSOL PROCESSES

In order to compare the importance of each kernel relative to another, it is convenient to convert Equation (13) into the following moment equation[1]:

$$\frac{d}{dt}\left(\int_0^\infty n(x,t)dx\right) = -\frac{1}{2}\int_0^\infty n(x,t)\int_0^\infty n(\xi,t)\phi(x,\xi)\,d\xi\,dx\,. \qquad (14)$$

Noting that Equation (14) has a form similar to the agglomeration equation for monodisperse aerosol systems, we now define the average collision kernel, $\bar{\phi}$, as

$$\bar{\phi} = \frac{\int_0^\infty n(x,t)\int_0^\infty n(\xi,t)\phi(x,\xi)\,d\xi\,dx}{\left(\int_0^\infty n(x,t)\,dx\right)^2}\,. \qquad (15)$$

Assuming aerosol size distributions remain lognormal as employed in the HAARM-3 code, the average Brownian, gravitational and turbulent kernels have been derived and are as follows:

$$\bar{K}_B = \frac{2}{3}\frac{kT}{\eta}\left(1 + \exp(\tfrac{1}{9}u) + A\exp(-\tfrac{1}{3}u + \tfrac{1}{18}\mu)\left[1 + \exp(\tfrac{2}{9}u)\right]\right) \qquad (16)$$

$$\bar{K}_G = \frac{2\pi g\rho}{9\eta}\cdot\exp(\mu+\tfrac{1}{2}u)\left(\exp(\tfrac{1}{3}\mu + \tfrac{1}{18}u)\left[\exp(\tfrac{1}{3}u)\,\mathrm{erf}(\tfrac{2\sqrt{u}}{3}) + 2\mathrm{erf}(\tfrac{\sqrt{u}}{3})\right]\right.$$
$$\left. + A\left[\mathrm{erf}(\tfrac{\sqrt{u}}{2}) + \exp(-\tfrac{2}{9}u)\,\mathrm{erf}(\tfrac{\sqrt{u}}{6})\right]\right) \qquad (17)$$

$$\bar{K}_T = \left(\frac{8\pi\,\varepsilon_T\rho_g}{15\eta}\right)^{1/2}\left(\exp(\mu+\tfrac{1}{2}u) + 3\exp(\mu+\tfrac{5}{18}u)\right) + 1.269\left(\frac{\rho}{\eta}\right)\left(\frac{\varepsilon_T^3\rho_g}{\eta}\right)^{1/4}$$
$$\cdot\exp(\mu+\tfrac{1}{2}u)\left(\exp(\tfrac{1}{3}\mu+\tfrac{1}{18}u)\left[\exp(\tfrac{1}{3}u)\,\mathrm{erf}(\tfrac{2\sqrt{u}}{3}) + 2\mathrm{erf}(\tfrac{\sqrt{u}}{3})\right]\right.$$
$$\left. + A\left[\mathrm{erf}(\tfrac{\sqrt{u}}{2}) + \exp(-\tfrac{2}{9}u)\,\mathrm{erf}(\tfrac{\sqrt{u}}{6})\right]\right) \qquad (18)$$

where

$$u = (3\ \ell n\ \sigma_g)^2$$

$$\mu = 3\ \ell n\ r_g$$

$$A = C_m\lambda\,.$$

Direct comparison of the magnitudes of $\overline{K}_B$, $\overline{K}_G$, and $\overline{K}_T$ is then equivalent to assessing the relative importance of each aerosol agglomeration mechanism. These are shown in Figure 4 for aerosol size distributions with various mass median radii and with geometric standard deviations of 1.5.

The regimes of predominance for these three agglomeration mechanisms can now be constructed and compared in a manner similar to that used for Figure 3. For this purpose, let us write the agglomeration equation for the monodisperse aerosol system:

$$\frac{dn}{dt} = -\overline{\phi} n^2 \tag{19}$$

where

$$\overline{\phi} = \overline{K}_B + \overline{K}_G + \overline{K}_T \ .$$

Solution of Equation (19) gives

$$\frac{n}{n_o} = \frac{1}{(1 + \overline{\phi} n_o t)} \ . \tag{20}$$

The time required for aerosol number concentration, n_o, to reduce to half of the initial concentration, or the half-life, is then

$$\frac{1}{2} = \frac{1}{(1 + \overline{\phi} n_o t_{50})}$$

or

$$t_{50} = \frac{1}{(\overline{K}_B + \overline{K}_G + \overline{K}_T) n_o} \ , \tag{21}$$

where t_{50} is the half-life.

In order to simplify the discussion, let us introduce the following dimensionless times

$$t'_{50} = \overline{\phi}_o n_o t_{50} \tag{22a}$$

$$t'_B = \overline{K}_{B,o} n_o t_{50} \tag{22b}$$

$$t'_G = \overline{K}_{G,o} n_o t_{50} \tag{22c}$$

$$t'_T = \overline{K}_{T,o} n_o t_{50} \tag{22d}$$

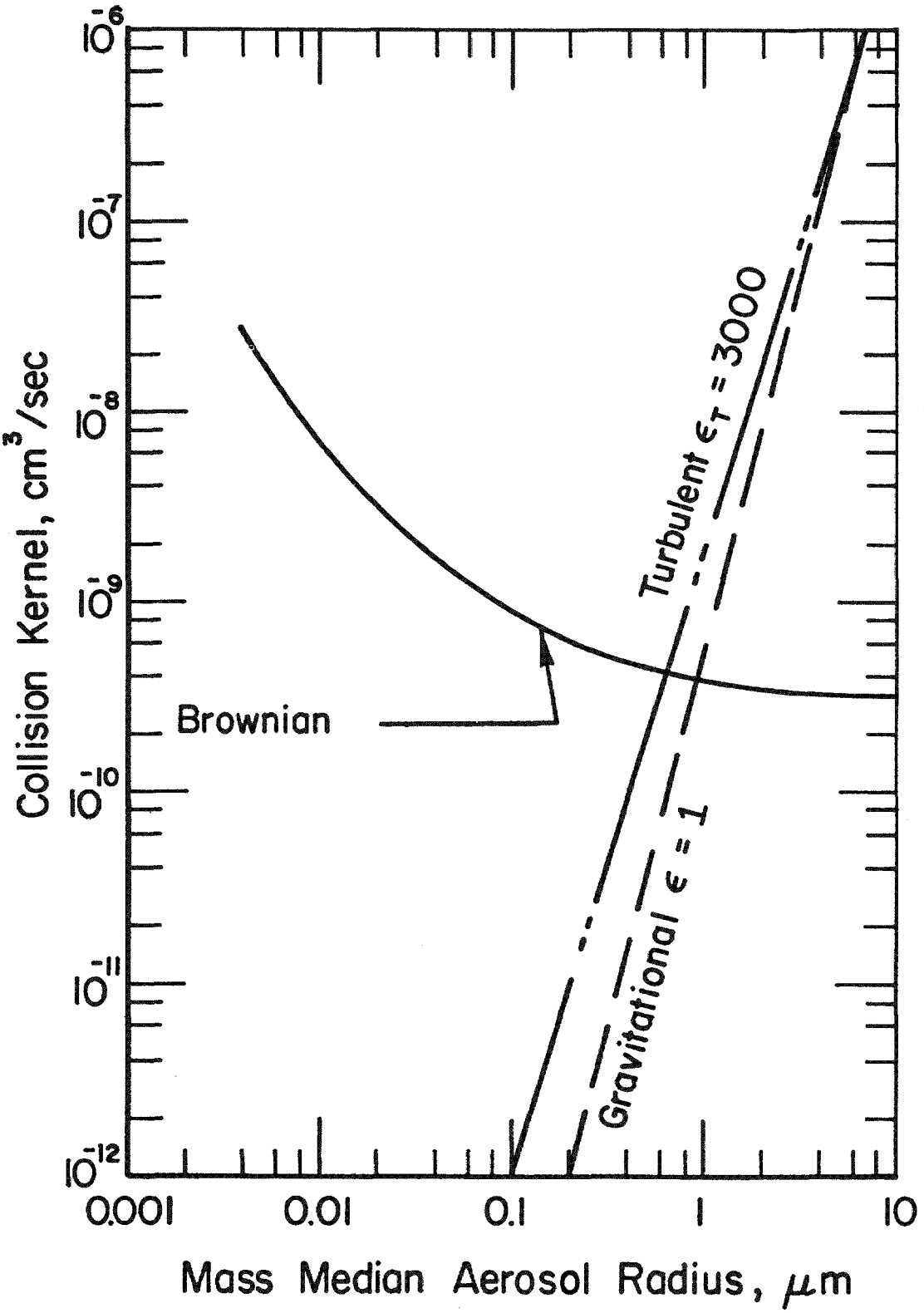

FIGURE 4. AVERAGE COLLISION KERNELS AS A FUNCTION OF THE MASS MEDIAN RADIUS FOR AEROSOLS OF LOGNORMAL DISTRIBUTION

where $K_{B,o}$, $K_{G,o}$ and $K_{T,o}$ are the average kernels at t = 0. Further, the dimensionless parameters standing for relative importance of each agglomeration mechanism may be defined as

$$BG = \overline{K}_{B,o}/\overline{K}_{G,o} \tag{23a}$$

$$TG = \overline{K}_{T,o}/\overline{K}_{G,o} \tag{23b}$$

$$BT = \overline{K}_{B,o}/\overline{K}_{T,o} \quad . \tag{23c}$$

Combining Equation (21), Equations (22) and Equations (23), the half-lives can be written as follows:

$$t'_B = 1/[1 + (1/BG) + (TG/BG)] \tag{24a}$$

$$t'_G = 1/[1 + BG + TG] \tag{24b}$$

$$t'_T = 1/[1 + (BG/TG) + (1/TG)] \quad . \tag{24c}$$

In order to construct the regimes of dominance, let us further consider the case in which one of three mechanisms is ignored and express the half-life in terms of the parameters defined in Equations (24). If Brownian agglomeration is ignored, $BG \to 0$ and $BT \to 0$, and we have

$$t'_G = 1/(1 + TG) \quad . \tag{25}$$

If gravitational agglomeration is negligible,

$$t'_T = 1/(1 + BT) \quad . \tag{26}$$

Similarly, if turbulent agglomeration is negligible,

$$t'_B = 1/(1+1/BG) \quad . \tag{27}$$

In constructing the domain of predominance, the criterion of whether values for t'_G, t'_T or t'_B, calculated using Equations (24), are larger than 90 percent of values for t''s calculated by Equations (25) to (27) may be used. Calculated regimes of controlling mechanisms based on the procedure just described are shown in Figure 5.

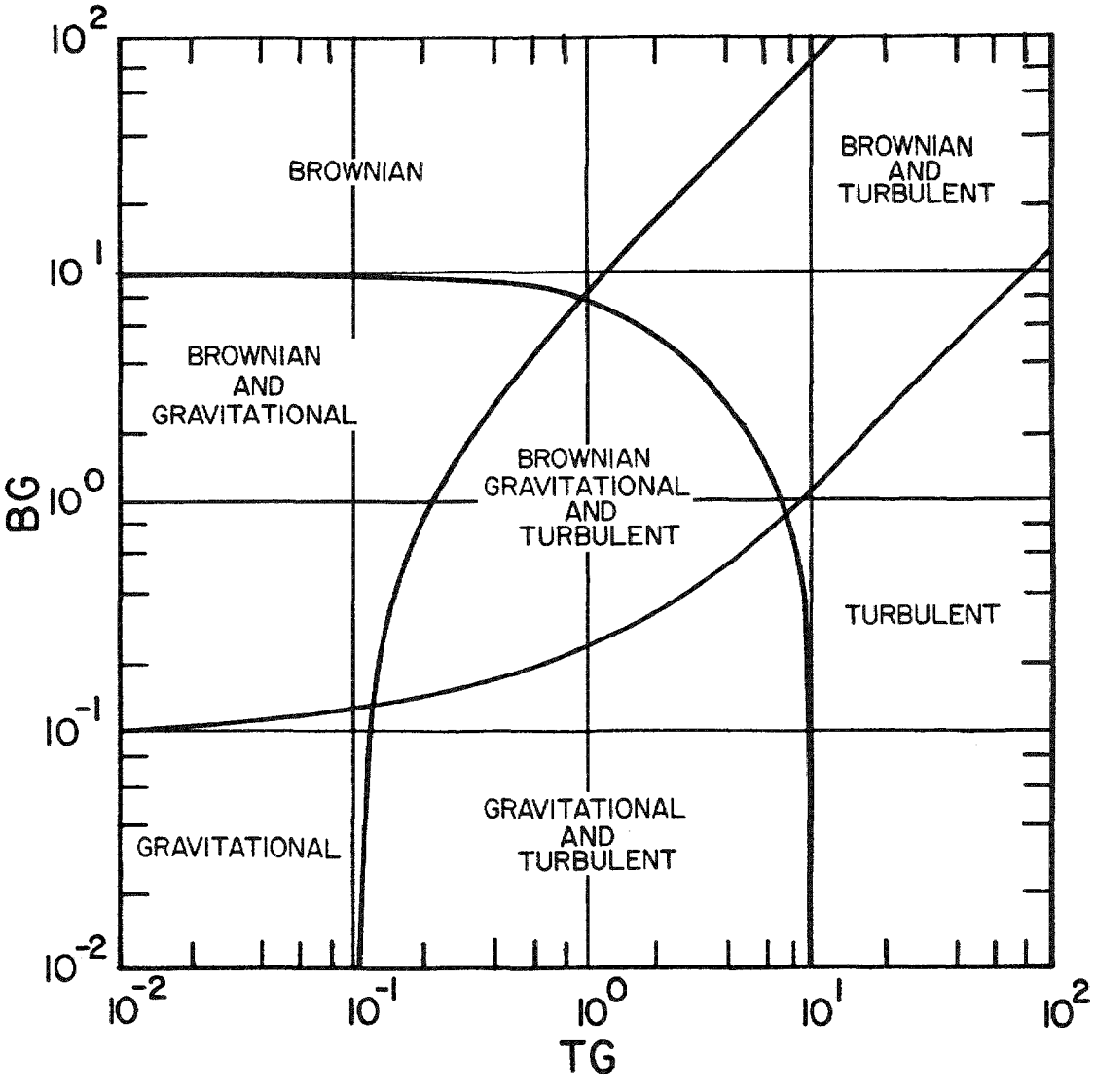

FIGURE 5. REGIMES OF IMPORTANCE FOR AGGLOMERATION KERNELS

The process for validating the agglomeration mechanisms included in the HAARM-3 computer code is to first identify the domains shown in Figure 3, which the postulated reactor accidents occupy, and then to perform appropriate experiments designed accordingly using similar values for the dimensionless parameters such as BG, TG and BT.

Procedure for Evaluating Importance of Deposition Mechanisms

Currently the HAARM-3 code contains three deposition mechanisms: Brownian diffusion, gravitational sedimentation and deposition due to thermophoretic forces. A procedure needed to validate these separate deposition mechanisms is provided as follows.

Assuming aerosols are monodisperse, let us write the governing equation describing the three deposition mechanisms as

$$\frac{dm}{dt} = - \frac{DA_w}{V\Delta} m - \frac{v_t}{H} m - \frac{A_w}{V} v_{th} m \quad , \tag{28}$$

where

m = aerosol mass concentration

v_{th} = thermophoretic deposition velocity.

The relative importance of the three aerosol deposition mechanisms will be compared by introducing the half-life which is defined as the time required for aerosol mass concentration, m, to reduce to half of the initial concentration. Since the solution of Equation (28) is

$$\frac{m}{m_o} = \exp \left[-\left(\frac{v_t}{H} + \frac{DA_w}{V\Delta} + \frac{A_w}{V} v_{th} \right) t \right] \quad , \tag{29}$$

the half life, t_{50}, is written

$$t_{50} = \ell n \; 2 / \left[\frac{v_t}{H} + \frac{DA_w}{V\Delta} + \frac{A_w}{V} v_{th} \right] \quad . \tag{30}$$

In addition to the dimensionless terms defined in Equations (10) to (12), let us define two additional terms involving the deposition velocity due to thermophoretic forces as

$$ThG = \frac{A_w v_{th}/V}{v_t/H} \tag{31}$$

$$DTh = \frac{D/\Delta}{v_{th}} \quad , \tag{32}$$

where ThG and DTh are the dimensionless terms showing relative importance of thermophoresis to sedimentation and that of diffusion to sedimentation respectively. Further, the following dimensionless terms for the half-life can be defined:

$$t'_{50} = (\frac{v_t}{H} + \frac{DA_w}{V} + \frac{A_w v_{th}}{V})t_{50} \tag{33a}$$

$$t'_D = (\frac{DA_w}{V\Delta})t_{50} \tag{33b}$$

$$t'_S = (v_t/H)t_{50} \tag{33c}$$

$$t'_{th} = (v_{th}A_w/V)t_{50} \quad . \tag{33d}$$

Combining Equations (30) to (33), the dimensionless half life can be written as follows

$$t'_D = \ell n2/[(1 + (1/DG) + (1/DTh)] \tag{34}$$

$$t'_S = \ell n2/[DG + 1 + ThG] \tag{35}$$

$$t'_{th} = \ell n2/[DTh + (1/ThG) + 1] \quad . \tag{36}$$

In order to construct the regimes of dominance, let us further consider the case in which one of three mechanisms is ignored and express the half-life in terms of the parameters defined in Equations (11), (31), and (32). If Brownian diffusion is negligible, $DG \to 0$ and $DTh \to 0$, and we have

$$t'_S = \ell n2/(1 + ThG) \quad . \tag{37}$$

If the gravitational sedimentation mechanism is negligible, $DG \to \infty$ and $ThG \to \infty$, so that

$$t'_{th} = \ell n2/(1 + DTh) \quad . \tag{38}$$

Similarly, if thermophoresis is negligible, $DTh \to \infty$, and $ThG \to 0$, and we have

$$t'_D = \ell n2/[1+(1/DG)] \ . \tag{39}$$

If the half life calculated by Equations (34) to (36) is larger than 90 percent of that calculated by, Equations (37) to (39), it can be assumed that the Brownian diffusion mechanism is not important. Similar criteria can be applied for the regimes in which gravitational sedimentation or thermophoresis is negligible. The resulting inequalities describing the above regimes are calculated to be

$$ThG > 9DG - 1 \tag{40}$$

$$DG > 9 - ThG \tag{41}$$

$$DG > -1 + 9ThG \ . \tag{42}$$

Inequalities (40) to (42) and the corresponding controlling aerosol deposition mechanisms are shown in Figure 6.

Special Considerations

In addition to the validation of correctness for individual and interacting mechanisms using results from experiments selected by the procedures described in the previous section, there are also special effects that must be considered. Such effects result from qualitative analysis of possible accident scenarios and conditions, and from consideration of the assumptions on which the HAARM-3 code is based. Likely to be of most importance are the following:

(1) Spatial inhomogeneity of aerosol concentration within the vessel

(2) Interaction rates among aerosols formed from different materials (e.g. fuel materials, structural materials, sodium oxides) and multiple size distribution modes (i.e., nonlognormal distributions)

(3) Characteristics of agglomerates formed from more than one material

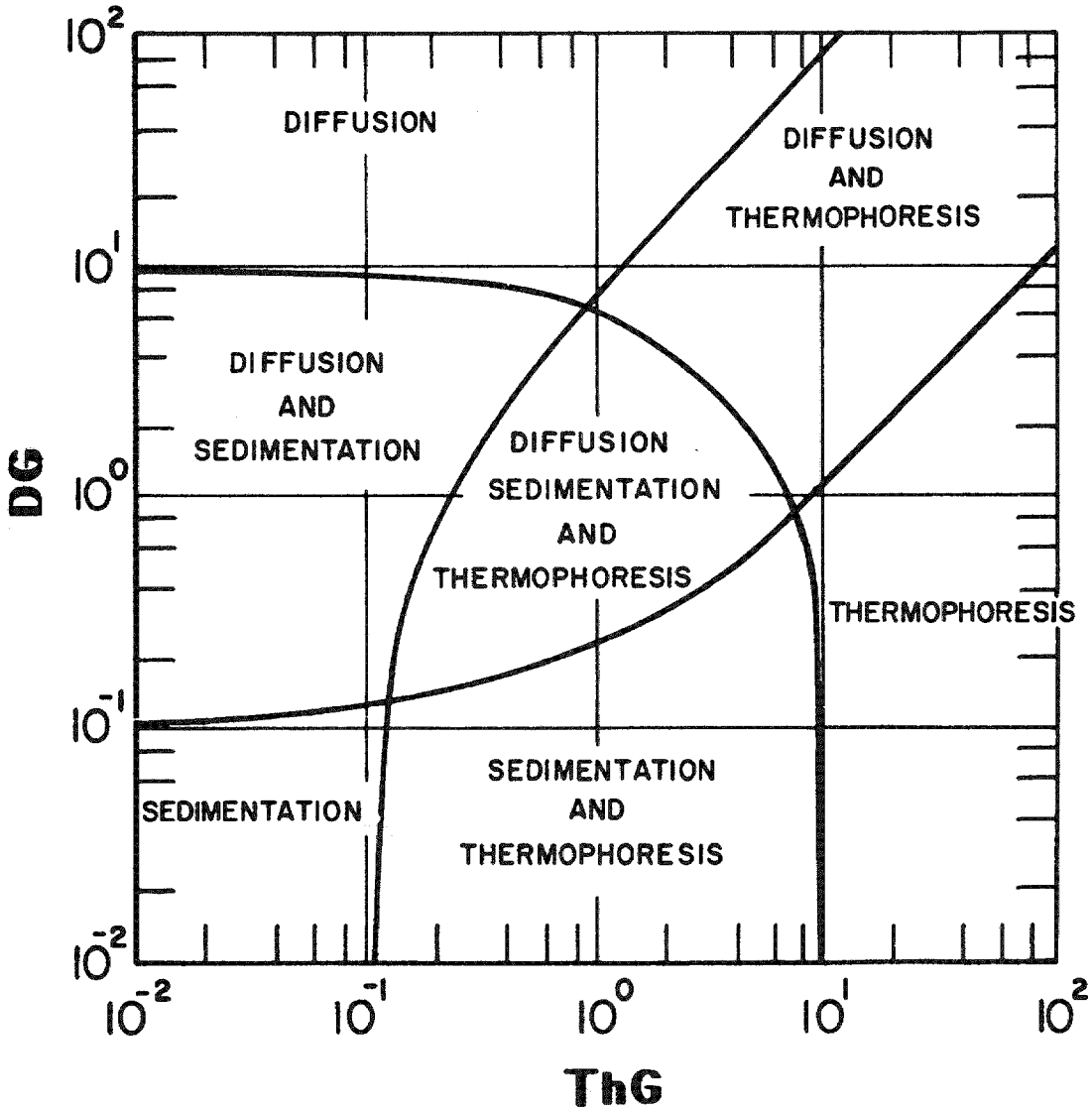

FIGURE 6. REGIMES OF IMPORTANCE FOR DEPOSITION PROCESSES

(4) Localized thermal effects that might alter deposition or sedimentation rates (e.g. heated vessel floor or surfaces leading to thermophoretic retardation of deposition)

(5) Heating or electrical charging of particles that affects agglomeration or deposition rates or that leads to resuspension

(6) Air flow patterns from changing thermal conditions or containment venting that could lead to resuspension.

The effects listed above are to a large extent associated with accident definitions. Experiments to validate the code for application to accident analyses must therefore be selected to include those effects believed to be significant for the various accident scenarios or conditions. The experiments must be selected to determine if these effects are significant or if mechanisms such as resuspension should be added to the code to make it a valid analysis tool.

EXPERIMENTAL CONDITIONS NEEDED FOR VERIFICATION

Selection of experimental conditions must be made on the basis of individual mechanism verification over the range of expected accident conditions and must account for the special considerations noted. The selection process must proceed first with an analysis of the estimated accident conditions to identify ranges for dimensionless groups and individual parameters that must be considered.

Analysis of Expected Accident Conditions

The estimated accident conditions were given previously in Table 1. From these conditions, the dimensionless parameters describing general aerosol behavior, CG and DG, can be calculated and then evaluated by using the procedures based on Figure 3. In addition, the conditions affecting

agglomeration mechanisms alone can be evaluated. To proceed with the evaluation, Table 4 was prepared in calculating values for the dimensionless groups CG and DG as defined by Equations (10) and (11). Because of uncertainties in values for the wall plating parameter, Δ, a range from 10^{-2} to 10^{-4} cm was considered. Similarly, although the maximum mass concentration was given in Table 1 as very high values, it is instructive to look at a range for maximum mass concentrations that goes to values as small as 10^{-4} times those listed. These ranges define regimes for CG and DG that correspond to the estimated accident conditions. These ranges for two particle size cases and for the various reactor volumes are shown in Figure 7.

As seen in Figure 7 all of the estimated accident conditions lead to aerosol behavior regimes where gravitational settling and agglomeration predominate. The obvious exception to this is the case of the smaller particles in the CRBR annular confinement volume (Identification No. 3-A). Since it is likely that aerosols in such a confinement volume would be subjected to removal by a gas cleaning system, such as a filter, which would in itself predominate, it is reasonable to exclude this volume from consideration.

The two particle size cases, A and B, represent approximate conditions at the beginning of an accident and after some time when the aerosol is aged. All points in this time evolution of the aged aerosol could represent conditions that would give pertinent regimes on Figure 7 to the right of the agglomeration controlling boundary and beneath the diffusional deposition region. This leads to the conclusion that aerosol behavior under estimated accident conditions is controlled by agglomeration and sedimentation. Therefore, experiments with Na_2O_x aerosols for code validation should emphasize conditions where sedimentation and agglomeration are the controlling factors.

A similar evaluation for fuel aerosols leads to the values for DG and CG presented in Table 5. From the values for these dimensionless groups it is evident that agglomeration and perhaps a combination of diffusional deposition and agglomeration would predominate. It can be concluded then, that experiments with aerosols formed from fuel materials should be designed to emphasize agglomeration and perhaps diffusional deposition.

TABLE 4. PREDOMINANT Na_2O_x AEROSOL BEHAVIOR REGIMES FOR ASSUMED ACCIDENTS

Ident. No.	Max Potent. Mass Conc., g/m^3 (a)	Max No. Conc. (n_o), p/cm^3(a,b)	H or $\left(\frac{A_F}{V}\right)^{-1}$, m	$\frac{A_W}{V}$, m^{-1}	CG	DG(c)
Case A, r_g = 0.25 μm						
1	2000	2.8×10^{10}	4	0.87	1.4×10^{6}	1.40
2	2000	2.8×10^{10}	38.5	1.1×10^{-1}	1.36×10^{7}	0.17
3	2.7	3.8×10^{7}	6.6	1.09	3.16×10^{3}	2.9
4	2000	2.8×10^{10}	28	0.121	9.9×10^{6}	1.36
5	2000	2.8×10^{10}	28	0.2	9.9×10^{6}	2.25
6	304	4.3×10^{9}	69	0.0867	3.74×10^{6}	2.40
Case B, r_g = 5 μm						
1	2000	3.5×10^{6}	4	0.87	0.44	1.7×10^{-4}
2	2000	3.5×10^{6}	38.5	1.1×10^{-1}	4.2	2.1×10^{-4}
3	2.7	4.8×10^{3}	6.6	1.09	1×10^{-3}	3.6×10^{-4}
4	2000	3.5×10^{6}	28	0.121	3.09	1.69×10^{-4}
5	2000	3.5×10^{6}	28	0.2	3.09	2.8×10^{-4}
6	304	5.4×10^{5}	69	0.0867	1.17	3.0×10^{-4}

(a) Range considered extends to 10^{-4} times these values.
(b) Assumes geometric standard deviation (σ) = 1.5.
(c) Values based on $\Delta = 10^{-3}$ cm. Values to 10 times these listed were considered for $\Delta = 10^{-4}$ cm.

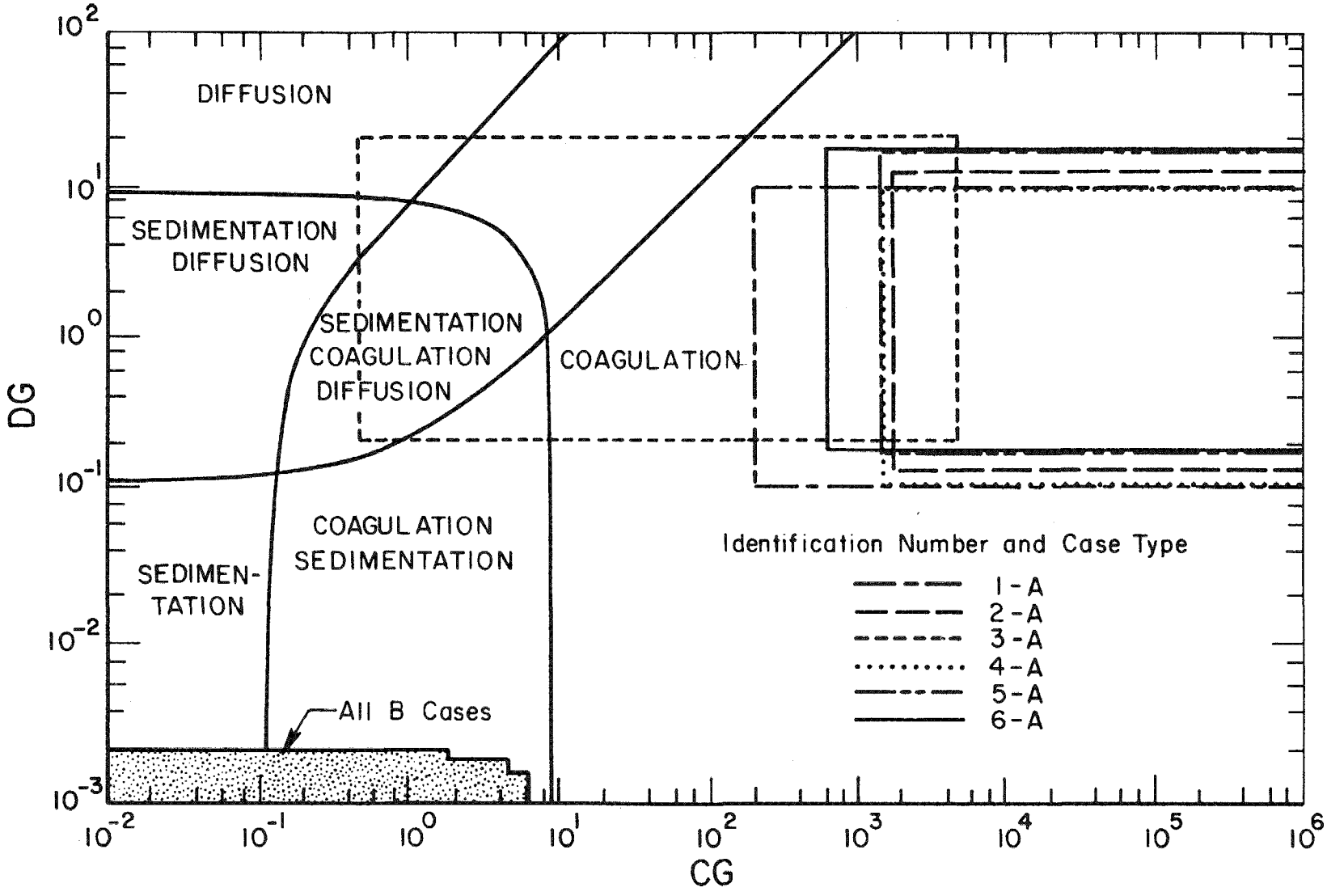

FIGURE 7. MECHANISMS CONTROLLING AEROSOL BEHAVIOR UNDER ESTIMATED ACCIDENT CONDITIONS

TABLE 5. PREDOMINANT FUEL AEROSOL BEHAVIOR REGIMES FOR ASSUMED ACCIDENTS

Ident. No.	Max Potent. Mass Conc., g/m^3 (a)	Max No. Conc, (n_o), p/cm^3 (a,b)	H or $\left(\frac{A_F}{V}\right)^{-1}$, m	$\frac{A_W}{V}$, m^{-1}	CG	DG(c)
1	282	1.6×10^{11}	4	0.87	7.8×10^{8}	5.6×10^{3}
2	1.9	1.08×10^{9}	38.5	1.1×10^{-1}	5.1×10^{9}	6.8×10^{3}
3	--	--	6.6	1.09	--	--
4	2.86	1.63×10^{9}	28	0.121	5.6×10^{7}	5.5×10^{3}
5	49	2.78×10^{10}	28	0.2	9.5×10^{8}	9.0×10^{3}
6	3.4	1.93×10^{9}	69	0.0867	1.6×10^{8}	9.6×10^{3}

(a) Range considered extends to 10^{-4} times these values.
(b) Assumes geometric standard deviation (σ) = 1.5.
(c) Values based on $\Delta = 10^{-3}$ cm. Values to 10 times these listed were considered for $\Delta = 10^{-4}$ cm.

Because of the importance of agglomeration for both Na_2O_x and fuel aerosols, it is crucial that the conditions leading to predominance of the various agglomeration mechanisms be evaluated. This can be done by using Figures 4 and 5 in addition to the analyses on which they are based. It is seen in Figure 4 that for small particle sizes (representative of fuel particles), Brownian agglomeration predominates. For larger particles, either gravitational or turbulent agglomeration can predominate depending on the estimated level of the turbulent energy dissipation rate.

To evaluate more specifically the importance of the various agglomeration mechanisms under expected accident conditions, Figure 5 can be used. For this analysis, an estimated range for the turbulent energy dissipation rate must be assumed. This has been chosen as $10 < \varepsilon_T < 10{,}000$ cm^2/sec^3. Assuming sodium oxide aerosols and using the particle sizes of 0.25 and 5 μm, standard conditions for gas density and viscosity, and a particle density of 2.27 g/cm^3, ranges of expected values for the dimensionless groups BG and TG have been calculated. The dimensionless groups BG and TG are as defined by Equations (23a) and (23b). For r_{50} = 0.25 μm, BG is 1.2×10^2 and TG ranges from 0.11 to 5.91. For r_{50} = 5 μm, BG is 9.19×10^{-4} and TG ranges from 2.22×10^{-2} to 3.13. The area encompassed within these ranges is shown in Figure 8.

It is seen from Figure 8 that all agglomeration mechanisms are expected to be significant at various stages of postulated accidents. The conditions during the agglomeration growth and deposition processes in an accident follow nearly vertical lines on Figure 8 from small particle sizes corresponding to large values for BG down to large sizes and low BG values. Proceeding along such a path, Brownian agglomeration predominates at first and as the particles grow, gravitational and turbulent agglomeration become predominant. Of course, the extent to which gravitational and turbulent become significant depends on the extent of particle growth. For the expected accident conditions given in Table 4, considerable growth is expected.

Similar observations can be made for the cases involving fuel aerosols with the only significant difference being the extent of particle

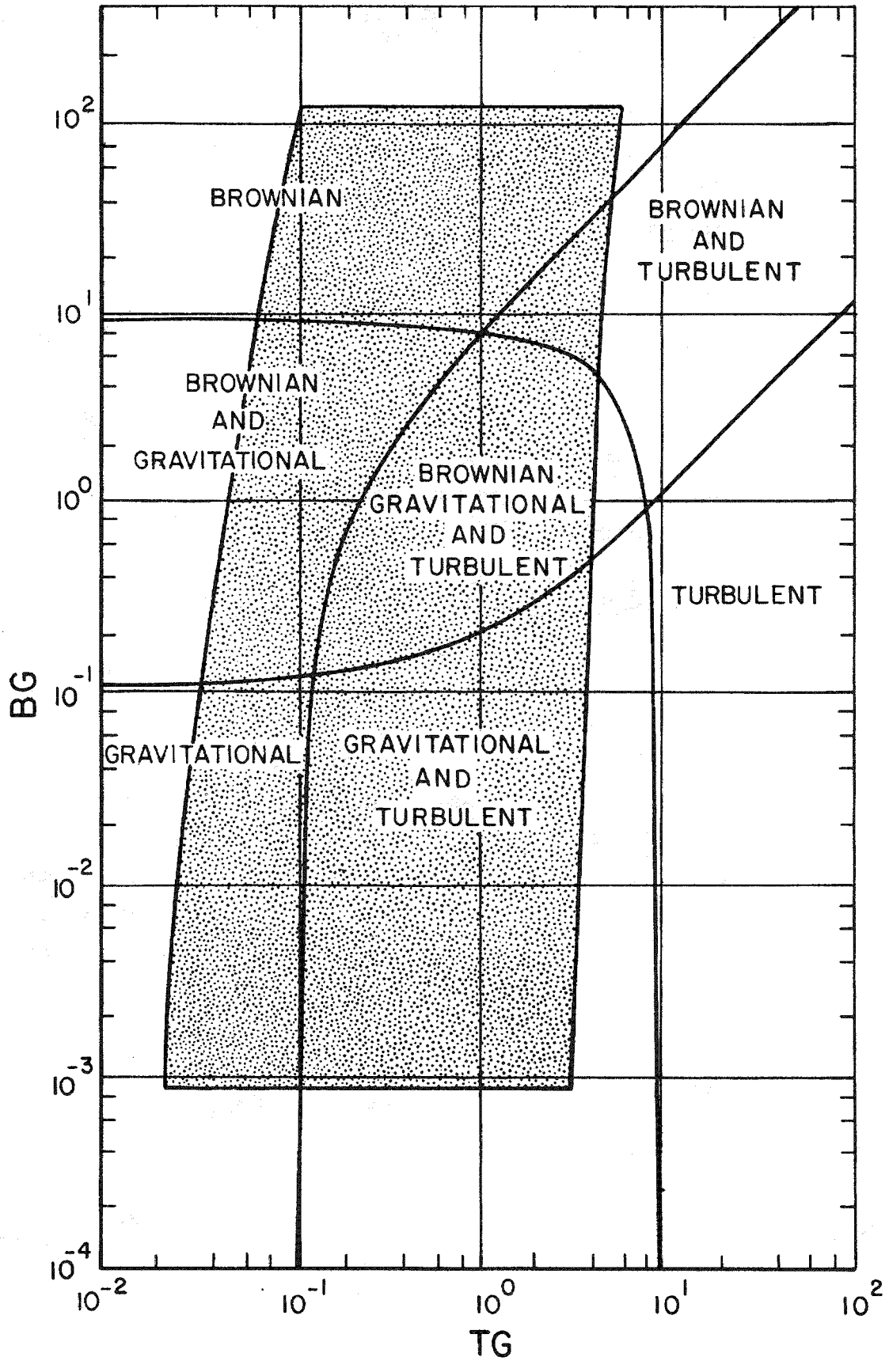

FIGURE 8. CONTROLLING AGGLOMERATION MECHANISMS UNDER ESTIMATED ACCIDENT CONDITIONS

growth. Particle sizes in excess of 1 μm can be expected to be grown in most cases but, of course, this size will vary somewhat depending on source strength and vessel geometry. For particles larger than 1 μm, it can be shown, however, that all agglomeration mechanisms can be of some significance.

A final comparison of rate mechanisms can be made for the aerosol deposition processes. These comparisons have been made using the dimensionless groups DG and ThG, as defined by Equations (11) and (31) which include consideration of sedimentation and wall deposition from diffusion and thermophoresis. The conditions and geometries presented in Table 4 for sodium oxide aerosols and for expected accident conditions were used, and ranges for the wall temperature gradient of $20 < \nabla T < 200$ K/cm and for the diffusional deposition layer of $10^{-4} < \Delta < 10^{-2}$ cm were assumed. For fixed geometry, concentration and particle size, these ranges define a rectangular region in the ThG/DG plane. The area swept by these rectangles for the various conditions and particle sizes is shown partially in Figure 9. The upper right region corresponds to a radius of 0.25 μm, and increasing particle size causes the points of interest to move toward the lower left part (the lowest region shown corresponds to a radius approaching 2.5 μm). The diffusion mechanism is significant when particle radius is less than about 1 μm, diffusion layer thickness is 10^{-4} cm, and the geometric term ($A_w H/V$) is large but can also be important over a range of geometries for particle radius approaching 0.25 μm. Thermophoresis predominates, however, for particle radii less than 1 μm when the geometric term is large over the range of ∇T and Δ values. For the expected accident conditions, a particle would be influenced by the following deposition mechanisms as a function of its growth: thermophoresis and possibly diffusion at r = 0.25 μm; sedimentation and thermophoresis through mid-range particle size with the predominant deposition mechanism shifting to sedimentation as the geometric term decreases; to a point (below the bottom left of the shaded curve) where sedimentation dominates for any of the ranges of ∇T, Δ or geometric terms as particle radius approaches 5.0 μm.

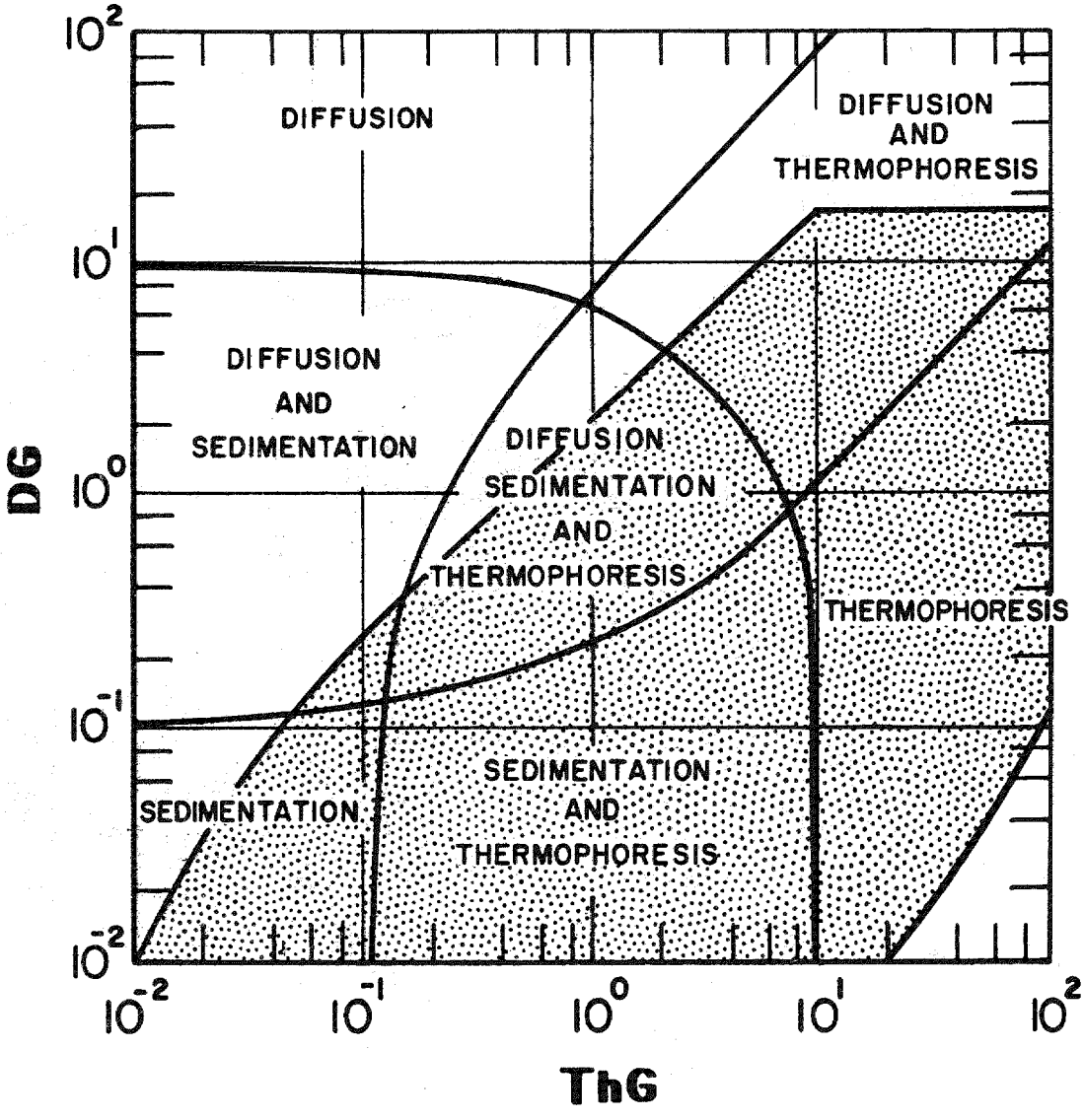

FIGURE 9. CONTROLLING DEPOSITION MECHANISMS UNDER ESTIMATED ACCIDENT CONDITIONS

Procedure for Selecting Experimental Conditions

The important variables for experimental study in the verification process are those identified by the sensitivity analysis which also are important in affecting agglomeration and sedimentation processes. As ranges for these variables are selected for consideration in experiments, it is important that the full selection of variables is such that the controlling processes are agglomeration, thermophoresis, and sedimentation by the mechanisms noted in the preceding analysis as being important. The crucial variables, exclusive of experiment geometry, are

(1) Particle size
(2) Aerosol mass concentration
(3) Aerosol material
(4) Turbulent energy dissipation rate
(5) Wall temperature gradient.

Other important parameters affecting agglomeration and sedimentation are those factors which correct for non-ideal behavior. These factors include α, the density correction; ε, the collision efficiency; χ, the mobility correction factor; and γ, the collision area factor. Since these factors cannot be controlled independently, they should be studied in separate effects experiments designed specifically for their determination. However, it is suggested that if necessary, contained aerosol behavior experiments be selected in addition to other experiments in order to provide some range in these factors.

The remaining factors of importance are those representing vessel geometry and the items discussed previously as special considerations. Vessel geometry is, of course, fixed by the various experimental facilities that have been used in the past or that are now available. By considering the specific sizes and configurations of these, the combinations of experimental variables and vessel dimensions must be used to choose values for DG and CG, BG and TG, and DG and ThG that cover the regimes representative of estimated accident conditions, and isolate the predominant mechanisms individually.

The expected ranges for specific variables and controlling mechanisms lead to specification of experimental conditions. These are given in Table 6.

TABLE 6. RECOMMENDED CONDITIONS FOR CONTAINED AEROSOL BEHAVIOR EXPERIMENTS

- VARIABLE SPECIFICATION

Variable	Range
1. Particle Size	0.02 - 10 μm
2. Aerosol Mass Concentration	0.2 - 200 g/m^3
3. Aerosol Material Density	2 - 12 g/m^3
4. Turbulent Energy Dissipation Rate	10 - 10,000

- DIMENSIONLESS GROUP SPECIFICATION

Na_2O_x $10^{-3} \leq DG \leq 10^{2}$ & $10^{2} \leq CG \leq 10^{6}$

$10^{-4} \leq DG \leq 10^{-1}$ & $10^{-4} \leq CG \leq 10^{2}$

with: $0.001 < BG < 100$ & $0.08 < TG < 6$

emphasizing: $DG < 20$ & $ThG < 0.08$

Fuel $10^{2} \leq DG \leq 10^{4}$ & $10^{3} \leq CG \leq 10^{8}$

with: $0.001 < BG < 10^{3}$ & $0.4 < TG < 15$

emphasizing: $DG < 20$ & $ThG < 100$

- SPECIAL CONSIDERATIONS

Conditions should be selected for additional experiments such that the items listed as special considerations can be checked.

- SEPARATE EFFECTS EXPERIMENTS

Special experiments should be used to validate code use of α, χ, γ, and ε.

EVALUATIONS OF SELECTED EXPERIMENTS

Although the recommended experimental conditions shown in Table 6 are intended for future experimental design considerations, it is of interest to evaluate past experiments to determine the extent to which results fall within the dimensionless group ranges for expected reactor accident conditions as determined by the HAARM-3 code. Figure 10 illustrates the maximum potential airborne concentration from both fuel and Na_2O_x aerosols as a function of reactor volume for each of the large scale reactor containment geometries given in Table 1. Also shown are the maximum potential airborne concentrations identified from a number of test vessel experiments. As indicated in Figure 10, past experiments have included a variety of vessel geometries from which a wide range of maximum potential airborne concentrations were determined. Experimental data from three such test facilities were chosen for evaluation using the HAARM-3 code dimensionless parameters. Test facilities were selected to encompass the range of maximum potential airborne concentrations and geometries; they included CSTF and NSPP, two facilities which are currently performing reactor accident testing, and LTC, from which two runs, Nos. 3 and 5, covering the extremes of maximum potential airborne concentrations, were selected.

The relative importance of coagulation, diffusion, and sedimentation mechanisms were discussed previously as they apply to large scale facilities. Agglomeration and gravitational settling were identified as the predominant behavior mechanisms of Na_2O_x aerosols for a range of particle sizes as shown in Figure 7. Figure 11 includes the ranges of conditions for expected accidents and also includes the resulting dimensionless parameters CG and DG determined from experimental data from CSTF, NSPP and LTC tests assuming a value of $\Delta = 10^{-3}$ cm. Results clearly show that these experiments were performed under conditions such that coagulation dominates in the range of small particle radius and gravitational settling dominates for particle radius approaching 5.0 μm; and that such results fall approximately within the limits of CG and DG values determined for large scale reactor accident conditions.

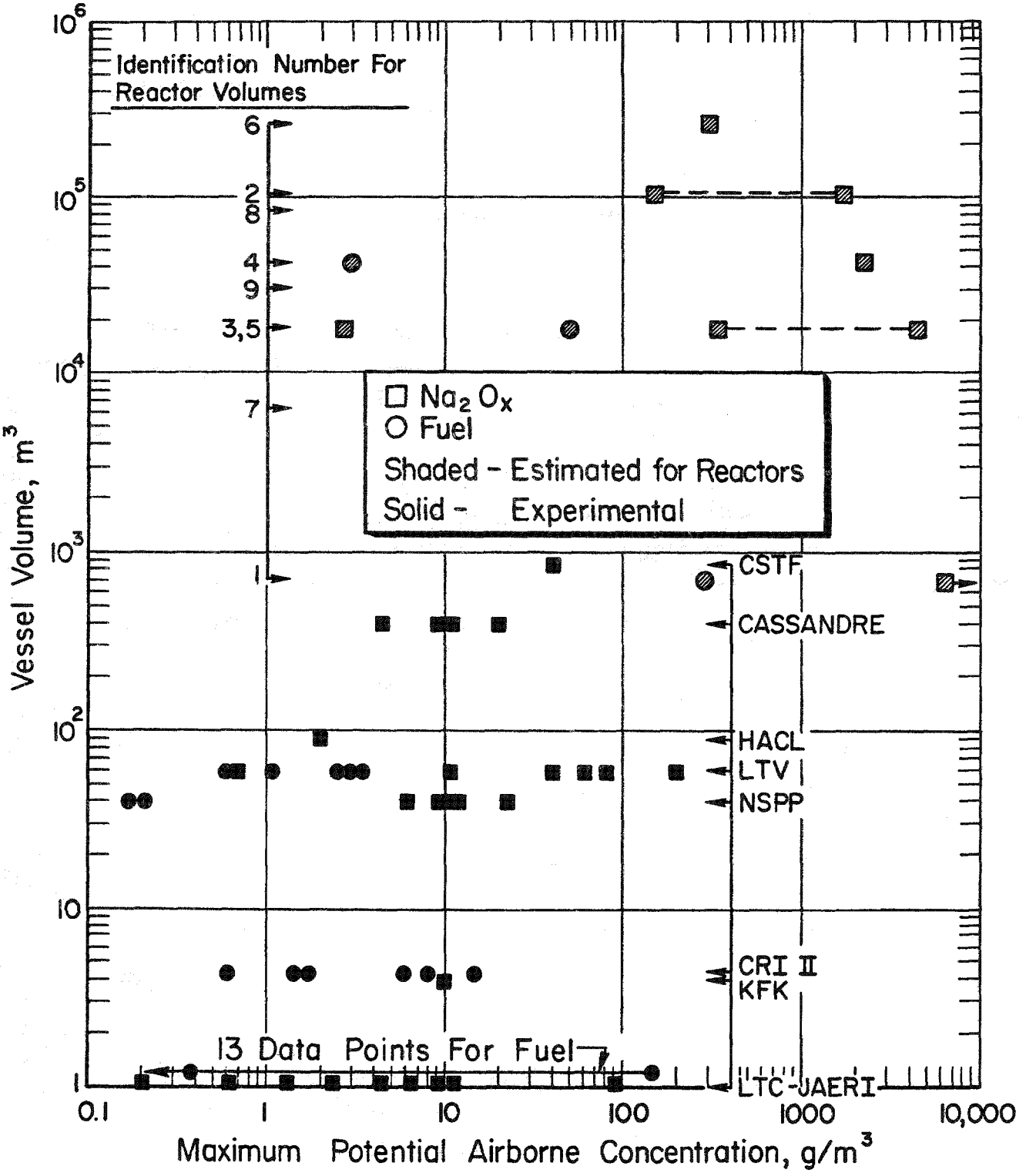

FIGURE 10. COMPARISON OF AEROSOL CONCENTRATIONS FOR EXPERIMENTAL AND POSTULATED ACCIDENT CONDITIONS

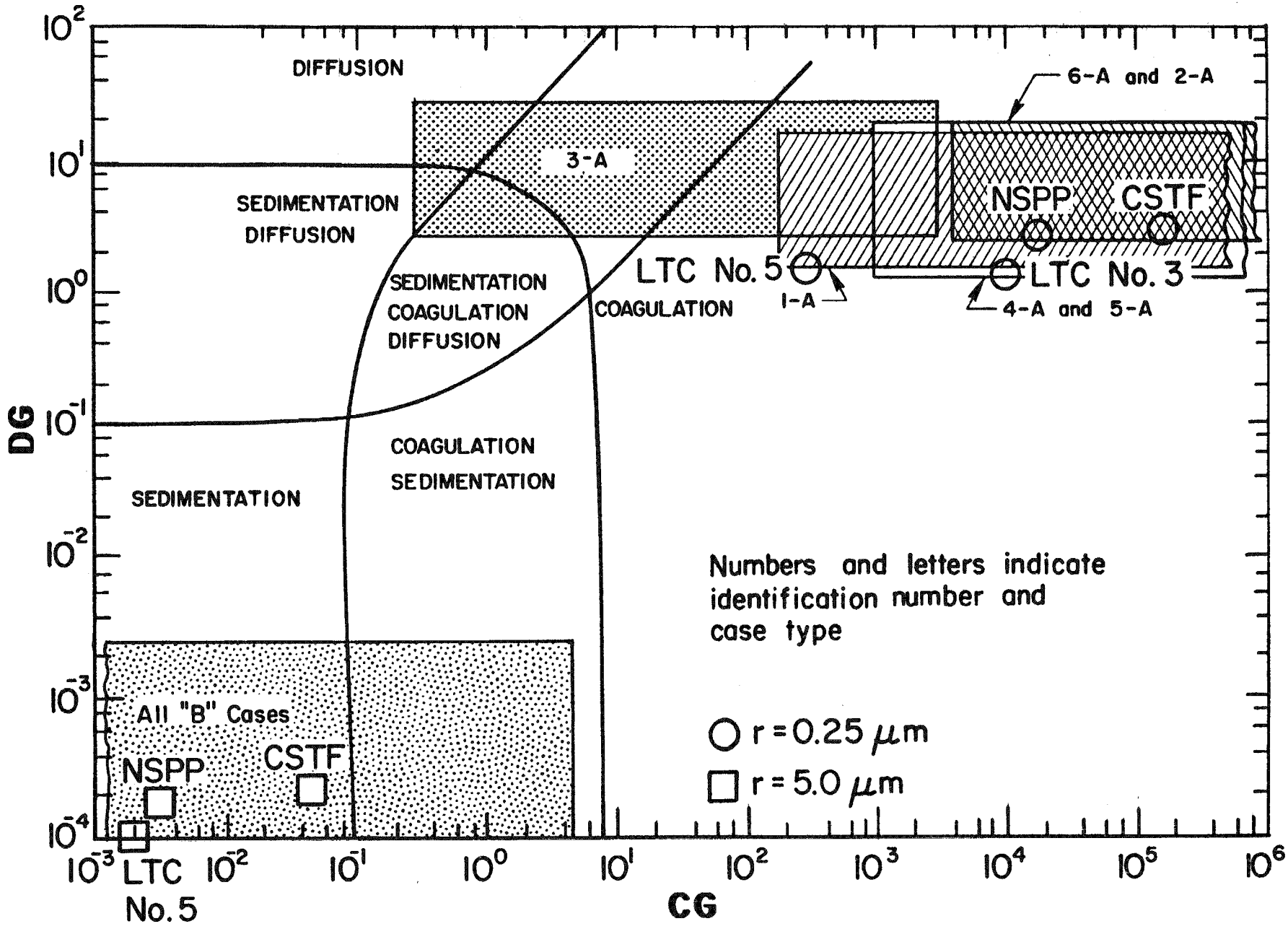

FIGURE 11. CONTROLLING MECHANISMS FOR SELECTED EXPERIMENTS

In evaluating the importance of agglomeration mechanisms in aerosol removal, Figure 9 was constructed to indicate regions of significance for large scale vessels under anticipated reactor accident conditions. As previously discussed, thermophoresis and possibly diffusion are predominant mechanisms for agglomeration under conditions of small particle size and large geometric term, whereas sedimentation predominates over the range of geometric, ∇T and Δ values as particle radius approaches 5 μm. Resulting DG and ThG values for CSTF, NSPP and LTC experiments, assuming $\Delta = 10^{-3}$ cm and $\nabla T = 40$ C/cm, are shown in comparison with values for expected accident conditions in Figure 12. Results based upon these assumptions confirm that tests were run under conditions where thermophoresis predominates for small particle sizes and sedimentation predominates for large particle size, and that results are consistent with DG and DTh findings for estimated reactor accident conditions when the geometric term is large, as is the case for CSTS, NSPP and LTC geometries ($A_w H/V$ ranges from approximately 5 to 11 for these facilities).

Future experiments will require that the selected test conditions result in dimensionless parameters consistent with those found necessary from the analyses of expected accident conditions and having values covering the predominance of all mechanisms. Because the use of such dimensionless groups achieves an independence of scale in aerosol behavior determinations under accident conditions, the agreement between experimental findings and code predictions may be directly assessed. Furthermore, the degree to which predictions and experiments agree when such parameters are used dictates the agreement to be expected between code predictions and actual aerosol behavior in full scale assemblies under anticipated accident conditions.

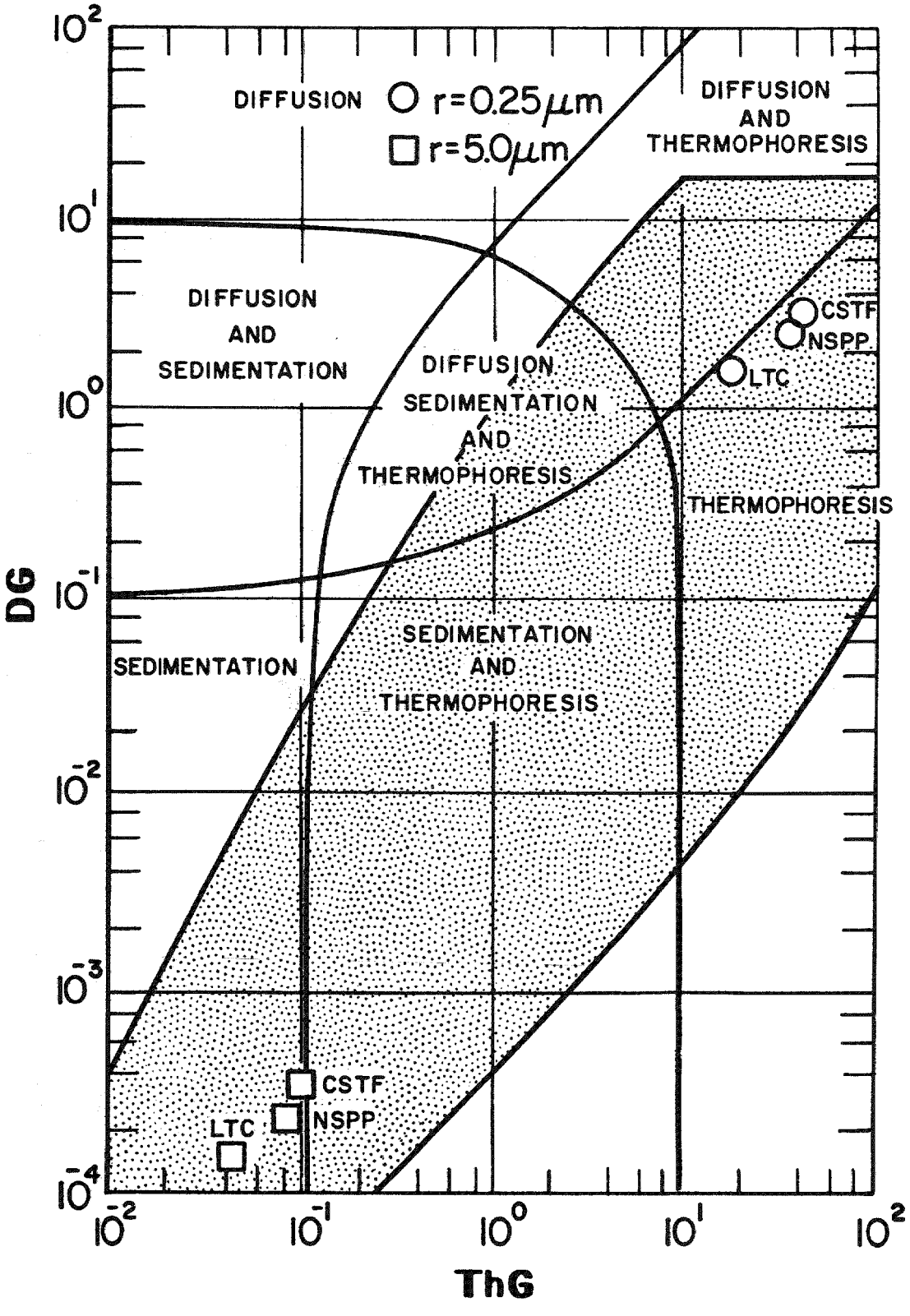

FIGURE 12. DEPOSITION MECHANISM IMPORTANCE FOR EXPERIMENTAL AND POSTULATED CONDITIONS

VERIFICATION REQUIREMENTS

The goal of this plan was to provide a procedure for validation of the HAARM-3 code by comparison with experiments such that predictions for full scale reactors will be possible with a high degree of confidence. Validation requirements are then needed to specify the extent and frequency of satisfactory agreement between code predictions and experimental results that will give the required degree of confidence that predictions for full scale systems will be within a selected uncertainty interval.

The validation procedure outlined in this plan is predicated on the premise that if the physical mechanisms controlling aerosol behavior have been properly identified, then experiments performed with variables and mechanisms chosen to match those expected for full scale conditions will provide a direct measure of aerosol behavior at full scale. This means that the verification procedure becomes one of direct comparisons between the predictions and experimental results.

A rigorous analysis accounting for an uncertainty analysis of the HAARM-3 code with an analysis of data variance at selected times to give a statistical evaluation of the degree of confidence in the data/prediction agreement should be used. Such an analysis could be based on a testing method such as the Student T test or the Wilcoxon rank sum statistics combined with the union-intersection principle, to provide a measure of confidence that the underlying hypothesis is valid. Such analyses should be preceded by statistical evaluations of the data sets themselves to eliminate from further consideration those sets which are significantly deviant from the remainder of the data sets such that they are classified as not being valid. This method of comparing the HAARM-3 code with experimental data will give a measure of the degree of confidence one has in the validity of the hypothesis of HAARM-3/data equality.

ACKNOWLEDGMENT

The authors would like to acknowledge the contributions of C. S. Jarrett, P. A. Connick and M. P. Rausch.

REFERENCES

(1) Gieseke, J. A., Lee, K. W., and Reed, L. D., "HAARM-3 Users Manual", BCL report to NRC, BMI-NUREG-1991 (Jan., 1978).

(2) Gieseke, J. A., Reed, L. D., Jordan, H., and Lee, K. W., "Characteristics of Agglomerates of Sodium Oxide Aerosol Particles", BCL Topical Report to NRC, BMI-NUREG-1977 (Aug, 1977).

(3) Gieseke, J. A., et al., "Aerosol Measurements and Modeling for Fast Reactor Safety: Annual Report for FY1977, Task 7", BCL Report to NRC, BMI-NUREG-1989 (Dec, 1977).

(4) Reed, L. D. and Gieseke, J. A., "HAARM-2 Users Manual", BCL report to NRC, BMI-X-665 (Oct, 1975).

(5) Reed, L. D. and Gieseke, J. A., "HAARM-1 Users Manual", BCL report to NRC, BMI-X-658 (May, 1975).

(6) Hubner, R. S., Vaughan, E. U., and Baurmash, L., "HAA-3 Users Report", AI-AEC13038 (March, 1973).

(7) Lee, K. W., Gieseke, J. A., and Reed, L. D., "Sensitivity Analysis of the HAARM-3 Code", BCL report to NRC, NUREG/CR-0527 & BMI-2008 (Oct, 1978).

(8) Okuyama, K., Kousaka, Y., and Yoshida, T., "Behavior of Aerosols Undergoing Brownian Coagulation, Brownian Diffusion and Gravitational Settling in a Closed Chamber", J. Chem. Engr. Jpn., 9(2), 140-146 (1976).

NRC FORM 335 (7-77) U.S. NUCLEAR REGULATORY COMMISSION

BIBLIOGRAPHIC DATA SHEET

1. REPORT NUREG BMI

2. (Leav

3. RE

DO NOT MICROFILM

4. TITLE AND SUBTITLE *(Add Volume No., if appropriate)*

HAARM-3 CODE VERIFICATION PROCEDURE

5. DA... MONTH October

7. AUTHOR(S)

J. A. Gieseke, K. W. Lee, H. Jordan, and H. A. Arbib

9. PERFORMING ORGANIZATION NAME AND MAILING ADDRESS *(Include Zip Code)*

Battelle Columbus Laboratories
505 King Avenue
Columbus, OH 43201

DATE REPORT ISSUED

MONTH: November YEAR: 1982

6. *(Leave blank)*

8. *(Leave blank)*

12. SPONSORING ORGANIZATION NAME AND MAILING ADDRESS *(Include Zip Code)*

Division of Reactor Safety Research
Office of Nuclear Regulatory Research
U.S. Nuclear Regulatory Commission
Washington, DC 20555

10. PROJECT/TASK/WORK UNIT NO.

11. CONTRACT NO.

A4063

13. TYPE OF REPORT

Topical Report

PERIOD COVERED *(Inclusive dates)*

15. SUPPLEMENTARY NOTES

14. *(Leave blank)*

16. ABSTRACT *(200 words or less)*

A procedure is provided for verifying experimentally the HAARM-3 aerosol behavior code. Methodology is obtained for selecting experimental conditions under which important aerosol agglomeration and deposition mechanisms can be separately evaluated. It is additionally suggested that a statistical analysis be employed to assess the level of significance with which the HAARM-3 model can predict experimental data.

17. KEY WORDS AND DOCUMENT ANALYSIS

17a. DESCRIPTORS

LMFBR
aerosol
sodium oxide
uranium oxide
particles

17b. IDENTIFIERS/OPEN-ENDED TERMS

18. AVAILABILITY STATEMENT

Unlimited

19. SECURITY CLASS *(This report)* Unclassified

21. NO. OF PAGES 55

20. SECURITY CLASS *(This page)* Unclassified

22. PRICE $